MODELING OF IN SITU NEUTRALIZATION AND BIODEGRADATION PROCESSES AND NUMERICAL SIMULATION WITH THE THREE-POINT BACKWARD FINITE DIFFERENCE METHOD

by

JIANCHU WU

B.S., ChE, Tianjin University, Tianjin, China. 1982

A MASTER'S THESIS

submitted in partial fulfillment of the

requirement of the degree

MASTER OF SCIENCE

Department of Chemical Engineering

KANSAS STATE UNIVERSITY

Manhattan, Kansas

1989

Approved by:

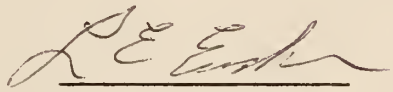

L. E. Erickson
Major Professor

In memory of my late father,

Mr. Chi Wu,

to whom this work is dedicated.

TABLE OF CONTENTS

ACKNOWLEDGEMENT.....i

CHAPTER 1 INTRODUCTION.....1-1

CHAPTER 2 THREE-POINT BACKWARD FINITE DIFFERENCE METHOD FOR CONVECTION-DISPERSION PARTIAL DIFFERENTIAL EQUATIONS.....2-1

2.1 ALGORITHM FOR A PDE WITH LINEAR REACTION TERM.....2-4

2.1.1 Three-Point Backward Difference Formulation.....2-5

2.1.2 Derivation of the Scheme.....2-6

2.1.3 Starting Algorithm.....2-9

2.1.4 Stability.....2-11

2.1.5 Example.....2-11

2.2 ALGORITHM FOR PDE's WITH COUPLED NONLINEAR REACTION TERMS.....2-13

2.2.1 Two-Step Expansion of Nonlinear Reaction Terms.....2-13

2.2.2 Uncoupling PDE's with Coupled Nonlinear Reaction Terms.....2-16

2.2.3 Uncoupling PDE's coupled with ODE's and/or Algebraic Equations.....2-17

2.2.4 Example.....2-18

2.3 CONCLUDING REMARKS.....2-19

REFERENCES.....2-23

CHAPTER 3 MODELING AND SIMULATION OF IN SITU NEUTRALIZATION PROCESSES.....3-1

3.1 MECHANISMS OF SOIL NEUTRALIZATION.....3-2

3.2 MODEL DESCRIPTION AND EQUATIONS.....3-3

3.3 ADSORPTION/DESORPTION RELATIONS.....3-5

3.4 DIMENSIONLESS FORM OF GOVERNING EQUATIONS OF THE MODEL.....3-7

3.5 SOLUTION ALGORITHM.....3-9

3.6 RESULTS AND DISCUSSION.....3-11

3.6.1 Effect of St_m.....3-12

3.6.2 Effect of R_o.....3-14

3.6.3 Effect of $\bar{K}_p$.....3-15

3.7 CONCLUDING REMARKS.....3-16

NOTATION.....3-23

REFERENCES.....3-24

CHAPTER 4 MODELING AND SIMULATION OF IN SITU BIODEGRADATION PROCESSES.....4-1

4.1 MODEL DEVELOPMENT.....4-2

4.1.1 Assumptions.....4-3

4.1.2 Derivation of a General Model.....4-4

4.1.3 Derivation of a Nonequilibrium Model....4-7

4.1.4 Dimensional Analysis.....4-10

4.2 SOLUTION ALGORITHM.....4-14

4.3 RESULTS AND DISCUSSION.....4-19

4.3.1 Dynamics of the Once-Through Operation..4-19

4.3.2 Dynamics of the recycling operation.....4-21

4.4 CONCLUDING REMARKS.....4-23

NOTATION.....4-24

REFERENCES.....4-26

CHAPTER 5 CONCLUSIONS AND RECOMMENDATIONS.....5-1

5.1 CONCLUSIONS.....5-1

5.2 RECOMMENDATIONS.....5-3

REFERENCES.....5-6

APPENDIX I.....A-1

APPENDIX II.....A-2

ACKNOWLEDGEMENT

The author wishes to express his sincere gratitude to Dr. L. E. Erickson, Professor of Chemical Engineering, for his continuous guidance through the author's degree study. Special thanks are due to Dr. L. T. Fan, University Distinguished Professor and Head of Chemical Engineering, for his valuable advice and guidance through the preparation of this thesis. Thanks are also due to Dr. Q. Zou and Dr. K. Halasi, Assistant Professors of Mathematics, for their valuable comments.

A special gratitude is to his wife, Yen Lee, for her love, encouragement and support.

Although the research described in this thesis has been funded in part by the United States Environmental Protection Agency under assistance agreement R-815709 to the Hazardous Substance Research Center for U. S. EPA Region 7 and 8 with headquarters at Kansas State University, it has not been subjected to the Agency's peer and administrative review and therefore may not necessarily reflect the views of the agency and no official endorsement should be inferred. This research was partially supported by the Kansas State University Office of Hazardous Waste Research.

CHAPTER 1

INTRODUCTION

The contamination of organic compounds in groundwater and soil has rapidly emerged as a world-wide environmental issue. There are a number of techniques available to remediate soil contaminated with organic compounds, including physical containment, in situ chemical treatment and in situ biological treatment. Among these techniques, in situ biodegradation, which treats organic contaminants by stimulating native microbial populations, has proven to be the most complete, cost-effective solution for ultimate cleanup of organic sludge.

The development of an in situ biodegradation process depends heavily upon the reaction kinetics and transport phenomena. The knowledge comes from not only laboratory experiments and field investigation, but also model development and numerical simulation. The latter is highly important in evaluating the treatment potential and optimizing the process design and operation. Moreover, it sheds light on the dynamics of cleanup processes, thereby showing insight into the progress of a biodegradation process.

One of the most important aspects of modeling and numerical simulation of biodegradation processes is the

numerical techniques for solving the model equations. In general, the mathematical model for a biodegradation process consists of several convection-dispersion partial differential equations (PDE's), which include the terms of accumulation, dispersion, convection and reaction. The dispersion is relatively small for the flow through porous media; thus, these PDE's are generally convection-dominated. The difficulty encountered in solving this type of PDE's numerically is that numerical oscillations and diffusion may adversely affect the accuracy of the numerical solution. Moreover, these PDE's couple one another through nonlinear reaction terms, and sometimes, they are also coupled with other ordinary differential equations (ODE's) or algebraic equations, thereby rendering the numerical techniques even more complicated. In Chapter 2, a new numerical method, the three-point backward finite difference method (TPB method), is derived for solving convection-dispersion PDE's. The method substantially reduces numerical oscillations and diffusion and is very effective in solving a system of PDE's with nonlinear reaction terms or a system of PDE's coupled with other ODE's or algebraic equations.

The first phase of an in situ bioremediation process is often an in situ neutralization process because an organic sludge is often an acid or base sludge. In Chapter 3, a mathematical model for in situ neutralization is developed.

The process features fast reaction and relatively slow adsorption/desorption, giving rise to a nonequilibrium model. The model equations consist of one PDE and two ODE's, and the TPB method developed in Chapter 2 is applied to solve these equations. Numerical simulation is conducted to show the effects of various parameters on the neutralization time and possible accumulation of base in the soil bed, which may convert the acidic soil into basic soil. Since an in situ neutralization process can be visualized as an in situ chemical treatment process, the model developed in this chapter can be extended to any other nonequilibrium system in which a contaminant deposited in a soil bed is to be eliminated with another chemical agent.

In comparison with the model for in situ chemical treatment, the model for in situ biological treatment is more complicated because it considers not only the fate of contaminants in soil, but also the effects of insufficient supply of nutrients and growth of microorganisms on the rate of biodegradation. Moreover, the rate of biodegradation may be limited by transport resistance to contaminant migration. In Chapter 4, a mathematical model for in situ biodegradation of organic sludge is developed. The model equations consist of three convection-dispersion PDE's and one ODE. The TPB method is employed to solve the model equations, and numerical simulation is performed to show the

effects of the model parameters on the rate of biodegradation. Furthermore, the recycle of unreacted contaminants is simulated, providing insight into the cleanup process as well as the information for process design and optimization.

The major conclusions drawn from the present study are summarized in Chapter 5. Some recommendations for future work are also outlined in this chapter.

CHAPTER 2

THREE-POINT BACKWARD FINITE DIFFERENCE METHOD FOR SOLVING A SYSTEM OF MIXED HYPERBOLIC-PARABOLIC PARTIAL DIFFERENTIAL EQUATIONS

The development and numerical solution of mathematical models that describe the dynamics of transport phenomena and reactions occurring in chemical process systems have received considerable attention. Mathematical modeling of a tubular flow system, e.g., a fixed-bed reactor or an adsorption bed, often results in a system of partial differential equations (PDE's) including the terms for accumulation, axial diffusion (dispersion), convection and reaction. These equations are termed mixed hyperbolic-parabolic PDE's (mixed PDE's) (see, e.g., Lapidus and Pinder, 1982); they are also known as convection-diffusion or convection-dispersion PDE's.

Mixed PDE's have conventionally been solved by finite difference methods. However, two major difficulties are encountered in applying the methods. The first is that most of the finite difference methods suffer from nonphysical numerical oscillations and excessive numerical diffusion (dissipation), and this becomes even more severe if mixed PDE's are convection-dominated (Finlayson, 1980; Allen et al., 1988). Consequently, the finite difference methods for

such equations have been considered to be suitable when large errors are tolerable (Khanna and Seinfeld, 1987). Numerous attempts have been made to improve the accuracy of finite difference methods for mixed PDE's and the focus has been on approximating the first-order temporal and spatial derivatives.

In approximating the first-order temporal derivative, the Euler method, based on forward or backward differencing, leads only to first-order temporal accuracy, and the Crank-Nicolson method, based on the trapezoidal formula, leads to second-order temporal accuracy. Obviously, the latter is more desirable than the former from the standpoint of accuracy; nevertheless, the Crank-Nicolson method has at least two major disadvantages. One is that the trapezoidal formula may result in a nondissipative scheme, i.e., the truncation error does not decay with the increase in time, even though the scheme is stable (Warming and Bean, 1978). The other is that this method induces unwanted finite oscillations near a point of discontinuity (see, e.g., Smith, 1985).

In approximating the first-order spatial derivative, the central difference formula tends to induce phase errors (Oran and Boris, 1987; Allen et al., 1988). The phase errors appear in the form of numerical oscillations (see, e.g., Finlayson, 1980; Smith, 1985). The upstream (upwind) formula

can eliminate the oscillations; however, it does so at the expense of numerical smearing at fronts that should, in fact, be sharp. This is caused by amplitude error, which appears in the form of numerical diffusion (Allen et al., 1988). The two types of error described here are of greatest concern when a PDE is convection-dominated.

In the first part of this chapter, three-point backward finite differencing (TPB) is introduced to approximate the first-order temporal and spatial derivatives in mixed PDE's. The temporal and spatial accuracy of the resultant method is of second order. It substantially reduces numerical oscillations and diffusion. Furthermore, the method generates a tridiagonal matrix on the left-hand side of the resultant finite difference equations; it is computationally efficient.

The second major difficulty encountered in applying a finite difference method to a system of mixed PDE's is caused by the coupled nonlinear reaction terms. A system of nonlinear finite difference equations is generated at each time step. Consequently, the tridiagonal matrix method, although highly efficient in solving linear finite difference equations, is not applicable for such a system. The common methods for solving these nonlinear finite difference equations are the quasi-linearization, Newton and

predictor-corrector methods. However, the first is of low-order accuracy, and the second or third requires iteration at each time step (see, e.g., Davis, 1984).

In the second part of this chapter, a two-step expansion technique is developed to linearize the finite difference equations and to uncouple the mixed PDE's; the accuracy of the expansion is of third order. Subsequently, the tridiagonal matrix method is applied to solve the resultant linear finite difference equations. The two-step expansion technique can be extended to uncouple a system of mixed PDE's coupled with ordinary differential equations (ODE's) and/or algebraic equations, thereby providing a highly effective technique for numerical simulation of complicated mathematical models.

2.1 ALGORITHM FOR A PDE WITH A LINEAR REACTION TERM

Let us consider the convection-diffusion mass transfer equation with a linear reaction term

$$\frac{\partial U}{\partial t} = D\frac{\partial^2 U}{\partial x^2} - v\frac{\partial U}{\partial x} - kU \tag{2.1}$$

Transforming this equation into the dimensionless form gives

$$\frac{\partial U}{\partial \theta} = \frac{1}{Pe}\frac{\partial^2 U}{\partial X^2} - \frac{\partial U}{\partial X} - \bar{k}U \tag{2.2}$$

where

$$\theta = \frac{tv}{L}, \quad X = \frac{x}{L}, \quad Pe = \frac{vL}{D}, \quad \bar{k} = \frac{kL}{v} \tag{2.3}$$

The appropriate initial and boundary conditions are (see, e.g., Wen and Fan, 1975)

$$\theta = 0, \quad U(0,X) = G(X) \tag{2.4}$$

$$X = 0, \quad U0 = \left(-\frac{1}{Pe}\frac{\partial U}{\partial X} + U\right)\Big|_{X=0^+} \tag{2.5}$$

$$X = 1, \quad \frac{\partial U}{\partial X} = 0 \tag{2.6}$$

where G(X) is a given function and U0 is a constant.

2.1.1 Three-Point Backward Difference Formulation

Finite difference methods resort to differencing to approximate the derivatives in a PDE. To formulate a second-order spatial derivative, the central differencing is well accepted and the spatial accuracy of this scheme is of second order. To express first-order temporal and spatial derivatives, the three-point backward (TPB) temporal differencing yields

$$\left(\frac{\partial U}{\partial \theta}\right)^{n+1} = \frac{3U^{n+1} - 4U^{n} + U^{n-1}}{2\Delta\theta} + O(\Delta\theta^2) \tag{2.7}$$

where superscript n stands for the n-th time step. Note that the TPB temporal differencing is a three time-level scheme; it has the same form as the two-step Gear method for initial-value ordinary differential equations. The TPB spatial differencing is expressed as

$$\left(\frac{\partial U}{\partial X}\right)_j = \frac{3U_j - 4U_{j-1} + U_{j-2}}{2\Delta X} + O(\Delta X^2) \tag{2.8}$$

where subscript j stands for the j-th grid point and j = 0, 1, ..., N. Note that the truncation error of both difference expressions is of second order.

2.1.2 Derivation of the Scheme

Application of the TPB differencing, equations (2.7) and (2.8), to approximate the first-order temporal and spatial derivatives in equation (2.2) yields

$$\frac{3U_j^{n+1} - 4U_j^n + U_j^{n-1}}{2\Delta\theta}$$

$$= \frac{1}{Pe}\left(\frac{\partial^2 U_j^{n+1}}{\partial X^2}\right) - \left(\frac{\partial U_j^{n+1}}{\partial X}\right) - \bar{k}U_j^{n+1} + O(\Delta\theta^2)$$

$$= \frac{1}{Pe}\left(\frac{U_{j+1}^{n+1} - 2U_j^{n+1} + U_{j-1}^{n+1}}{\Delta X^2}\right) - \frac{3U_j^{n+1} - 4U_{j-1}^{n+1} + U_{j-2}^{n+1}}{2\Delta X}$$

$$- \bar{k}U_j^{n+1} + O(\Delta\theta^2 + \Delta X^2) \qquad (2.9)$$

Rewriting this expression and ignoring the second-order truncation error result in

$$r_2 U_{j-2}^{n+1} - (r_1 + 4r_2)U_{j-1}^{n+1} + (3 + 2r_1 + 3r_2 + r_3)U_j^{n+1} - r_1 U_{j+1}^{n+1}$$

$$= 4U_j^n - U_j^{n-1} \qquad (2.10)$$

where

$$r_1 = \frac{2\Delta\theta}{Pe\Delta X^2} \qquad (2.11)$$

$$r_2 = \frac{\Delta\theta}{\Delta X} \qquad (2.12)$$

$$r_3 = 2\Delta\theta\,\bar{k} \qquad (2.13)$$

Equation (2.10) can be solved by the Gauss elimination method at each time step. It is highly desirable, however,

to form a tridiagonal matrix on the left-hand side of equation (2.10), thereby reducing the computational effort. To accomplish this, U_{j-2}^{n+1} on the left-hand side of equation (2.10) need be eliminated. Such a tridiagonal matrix can be generated by approximating the convection term with a "delta" form (Warming and Beam, 1978)

$$\Delta U^n = U^{n+1} - U^n \tag{2.14}$$

Rewriting equation (2.9) leads to

$$\begin{aligned}
&\frac{3U_j^{n+1} - 4U_j^n + U_j^{n-1}}{2\Delta\theta} \\
&= \frac{1}{Pe}\left(\frac{\partial^2 U_j^{n+1}}{\partial X^2}\right) - \left(\frac{\partial U_j^{n+1}}{\partial X}\right) + \left(\frac{\partial U_j^n}{\partial X}\right) - \left(\frac{\partial U_j^n}{\partial X}\right) - \bar{k}U_j^{n+1} + O(\Delta\theta^2) \\
&= \frac{1}{Pe}\left(\frac{\partial^2 U_j^{n+1}}{\partial X^2}\right) - \left(\frac{\partial}{\partial X}\right)\Delta U_j^n - \left(\frac{\partial U_j^n}{\partial X}\right) - \bar{k}U_j^{n+1} + O(\Delta\theta^2)
\end{aligned} \tag{2.15}$$

Subsequently, $\partial U_j^n/\partial X$ is approximated by the three-point backward formula, and $\partial \Delta U_j^n/\partial X$ is approximated by the upstream formula, thereby yielding

$$\begin{aligned}
&\frac{3U_j^{n+1} - 4U_j^n + U_j^{n-1}}{2\Delta\theta} \\
&= \frac{1}{Pe}\left(\frac{U_{j+1}^{n+1} - 2U_j^{n+1} + U_{j-1}^{n+1}}{\Delta X^2}\right) - \frac{\Delta U_j^n - \Delta U_{j-1}^n}{\Delta X} \\
&\quad - \frac{3U_j^n - 4U_{j-1}^n + U_{j-2}^n}{2\Delta X} - \bar{k}U_j^{n+1} + O(\Delta\theta^2 + \Delta X^2)
\end{aligned} \tag{2.16}$$

Ignoring the second-order truncation error and rewriting equation (2.16) give

$$(-r_1 - 2r_2)U_{j-1}^{n+1} + (3 + 2r_1 + 2r_2 + r_3)U_j^{n+1} - r_1 U_{j+1}^{n+1}$$
$$= -r_2 U_{j-2}^{n} + 2r_2 U_{j-1}^{n} + (4 - r_2)U_j^{n} - U_j^{n-1} \qquad (2.17)$$
$$2 \leq j \leq N-1$$

where r_1, r_2 and r_3 are defined in equations (2.11), (2.12) and (2.13), respectively. Equation (2.17) gives rise to the general finite difference expression for the TPB method. The accuracy of the method is of second order. Note that a tridiagonal coefficient matrix is generated on the left-hand side of equation (2.17).

For j = 1, $\partial U/\partial X$ is approximated by upstream scheme only, i.e.,

$$\frac{3U_1^{n+1} - 4U_1^{n} + U_1^{n-1}}{2\Delta\theta} = \frac{1}{Pe}\left(\frac{U_2^{n+1} - 2U_1^{n+1} + U_0^{n+1}}{\Delta X^2}\right) - \frac{U_1^{n+1} - U_0^{n+1}}{\Delta X}$$
$$- \bar{k}U_1^{n+1} + O(\Delta\theta^2 + \Delta X) \qquad (2.18)$$

To eliminate U_0^{n+1}, the boundary condition given by equation (2.5) is approximated by a three-point forward formula, thereby giving

$$U0 = -\frac{1}{Pe}\,\frac{-3U_0^{n+1} + 4U_1^{n+1} - U_2^{n+1}}{2\Delta X} + U_0^{n+1} \qquad (2.19)$$

or

$$U_0^{n+1} = 4r_4 U_1^{n+1} - r_4 U_2^{n+1} + r_5 \qquad (2.20)$$

where

$$r_4 = \frac{1}{3 + 2Pe\Delta X} \qquad (2.21)$$

$$r_5 = 2r_4 \Delta X \; Pe \; U0 \qquad (2.22)$$

Substitution of equation (2.20) into equation (2.18) yields

$$(3 + 2r_1 + 2r_2 + r_3 - 4r_1r_4 - 8r_2r_4)U_1^{n+1}$$
$$-(r_1 - r_1r_4 - 2r_2r_4)U_2^{n+1}$$
$$= 4\,U_1^n - U_1^{n-1} + (r_1 + 2r_2)r_5 \qquad (2.23)$$

For j = N, the boundary condition, equation (2.6), is approximated by the central difference formula,

$$\frac{U_{N+1} - U_{N-1}}{2\Delta X} = 0 \qquad (2.24)$$

and, therefore,

$$U_{N+1} = U_{N-1} \qquad (2.25)$$

Substituting this expression into equation (2.17) leads to

$$(-2r_1 - 2r_2)U_{N-1}^{n+1} + (3 + 2r_1 + 2r_2 + r_3)U_N^{n+1}$$
$$= -r_2U_{N-2}^n + 2r_2U_{N-1}^n + (4 - r_2)U_N^n - U_N^{n-1} \qquad (2.26)$$

The tridiagonal system of equations (2.17), (2.23) and (2.26) with unknown U_1 through U_N can be solved rapidly and stably by the tridiagonal matrix method (see, e.g., Smith, 1985). Then, U_0 can be obtained from equation (2.20).

2.1.3 Starting Algorithm

The TPB method is a three time-level method; thus, a starting algorithm is required to calculate U_j^1, j = 0, 1, ..., N. Moreover, the accuracy of the entire method will be influenced if the accuracy of the starting algorithm is not at least of second order. In the present work, the starting algorithm has been derived by combining the trapezoidal formula of temporal differencing and the three-point backward spatial differencing. The temporal and spatial

accuracy of the resultant method is of second order. Although it is nondissipative, the method is employed only for the first step. The derivation of the method is similar to that of the Crank-Nicolson method except that the first-order spatial derivative is approximated by the TPB differencing; it is given as follows:

$$\frac{U_j^{n+1}-U_j^n}{\Delta\theta}$$

$$= \frac{1}{2Pe}\left(\frac{\partial^2 U_j^{n+1}}{\partial X^2}\right) + \frac{1}{2Pe}\left(\frac{\partial^2 U_j^n}{\partial X^2}\right) - \frac{1}{2}\left(\frac{\partial U_j^{n+1}}{\partial X}\right) - \frac{1}{2}\left(\frac{\partial U_j^n}{\partial X}\right) - \frac{\bar{k}}{2} U_j^{n+1} - \frac{\bar{k}}{2} U_j^n + O(\Delta\theta^2)$$

$$= \frac{1}{2Pe}\left(\frac{U_{j+1}^{n+1} - 2U_j^{n+1} + U_{j-1}^{n+1}}{\Delta X^2}\right) + \frac{1}{2Pe}\left(\frac{U_{j+1}^{n} - 2U_j^{n} + U_{j-1}^{n}}{\Delta X^2}\right)$$

$$- \frac{1}{2}\frac{U_j^{n+1} - U_{j-1}^{n+1}}{\Delta X} - \frac{1}{2}\frac{3U_j^n - 4U_{j-1}^n + U_{j-2}^n}{2\Delta X}$$

$$- \frac{\bar{k}}{2} U_j^{n+1} - \frac{\bar{k}}{2} U_j^n + O(\Delta\theta^2+\Delta X^2) \qquad (2.27)$$

Note that $(\partial U/\partial X)^{n+1}$ is approximated through the upstream scheme to generate a tridiagonal matrix on the left-hand side of the finite difference equations. Rewriting equation (2.27) gives

$$(-s_1 - s_2)U_{j-1}^{n+1} + (1 + 2s_1 + s_2 + s_3)U_j^{n+1} - s_1 U_{j+1}^{n+1}$$

$$= -\frac{1}{2} s_2 U_{j-2}^n + (s_1 + 2s_2)U_{j-1}^n + (1 - 2s_1 - \frac{3}{2} s_2 - s_3)U_j^n + s_1 U_{j+1}^n$$

$$2 \leq j \leq N-1 \qquad (2.28)$$

where

$$s_1 = \frac{\Delta\theta}{2Pe\Delta X^2} \qquad (2.29)$$

$$s_2 = \frac{\Delta\theta}{2\Delta X} \tag{2.30}$$

$$s_3 = \frac{\Delta\theta\ \bar{k}}{2} \tag{2.31}$$

For j = 1 and j = N, the same treatment of the boundary conditions as equations (2.18) through (2.26) can be applied.

2.1.4 Stability

The TPB method is a three time-level implicit method; thus, it is unconditionally stable for a mixed PDE without a reaction term. Inclusion of the reaction term magnifies the complexity of the stability analysis; it varies from case to case. Nevertheless, the TPB method is more stable than the commonly used finite difference methods, such as the Crank-Nicolson and implicit Euler methods; the temporal differencing of the TPB method is identical to that of the two-step Gear method.

2.1.5 Example

The TPB method has been applied to the solution of the following convection-diffusion PDE;

$$\frac{\partial U}{\partial \theta} = \frac{1}{Pe}\frac{\partial^2 U}{\partial X^2} - \frac{\partial U}{\partial X} \tag{2.32}$$

In this example, Pe is considered to be 1000, thereby rendering the PDE to be convection-dominated. Equation

(2.32) has been solved subject to the following initial and boundary conditions, i.e.,

$$\theta = 0, \quad U(0,X) = 0 \tag{2.33}$$

$$X = 0, \quad U(\theta,0) = 1 \tag{2.34}$$

$$X = 1, \quad \frac{\partial U}{\partial X} = 0 \tag{2.35}$$

The resultant solution is given in Figure 2.1. For comparison, the solutions obtained with two conventional methods are also presented in the same figure (Finlayson, 1980). In contrast to the TPB method, the backward Euler method with the central differencing of the convection term causes appreciable numerical oscillations, and the backward Euler method with the upstream differencing of the convection term induces noticeable numerical diffusion. Note that the number of grid points is equal to 50 for all three methods; the time-step size is 0.01 for the TPB method and 0.0005 for the others. It is worth mentioning that the boundary condition at X=0, equation (2.34), is justifiable in the light of a relatively large Pe. The boundary condition satisfying the flux conservation, as given in Equation (2.5), yields essentially identical solutions to those obtained with equation (2.34).

2.2 ALGORITHM FOR PDE's WITH COUPLED NONLINEAR REACTION TERMS

In the preceding section, the TPB method for a mixed PDE with a linear reaction term has been developed. If we have a system of mixed PDE's with coupled nonlinear reaction terms, the method yields a system of nonlinear finite difference equations that need be solved at each time step. In this section, a two-step expansion technique is derived to convert the nonlinear finite difference equations into linear ones which can be solved with the tridiagonal matrix method.

2.2.1 Two-Step Expansion of Nonlinear Reaction Terms

The general form of a mixed PDE is

$$\frac{\partial U}{\partial \theta} = \frac{1}{Pe}\frac{\partial^2 U}{\partial X^2} - \frac{\partial U}{\partial X} + f(U) \qquad (2.36)$$

where f(U) is any given nonlinear function of U. Application of the TPB method to this equation yields

$$\frac{3U_j^{n+1} - 4U_j^n + U_j^{n-1}}{2\Delta\theta}$$

$$= \frac{1}{Pe}\left(\frac{\partial^2 U_j^{n+1}}{\partial X^2}\right) - \left(\frac{\partial U_j^{n+1}}{\partial X}\right) + f(U_j^{n+1}) + O(\Delta\theta^2)$$

$$= \frac{1}{Pe}\left(\frac{U_{j+1}^{n+1} - 2U_j^{n+1} + U_{j-1}^{n+1}}{\Delta X^2}\right) - \frac{\Delta U_j^n - \Delta U_{j-1}^n}{\Delta X}$$

$$- \frac{3U_j^n - 4U_{j-1}^n + U_{j-2}^n}{2\Delta X} + f(U_j^{n+1}) + O(\Delta\theta^2 + \Delta X^2) \qquad (2.37)$$

or

$$(-r_1 - 2r_2)U_{j-1}^{n+1} + (3 + 2r_1 + 2r_2)U_j^{n+1} - r_1 U_{j+1}^{n+1}$$
$$= -r_2 U_{j-2}^{n} + 2r_2 U_{j-1}^{n} + (4-r_2)U_j^{n} - U_j^{n-1} + 2\Delta\theta\, f(U_j^{n+1})$$
$$2 \leq j \leq n-1 \qquad (2.38)$$

where r_1 and r_2 are defined in equations (2.11) and (2.12), respectively. To solve equation (2.38) with the tridiagonal matrix method, $f(U_j^{n+1})$ can be approximated with the Taylor-series expansion, i.e.,

$$f(\theta + \Delta\theta) = f(\theta) + f'(\theta)\,\Delta\theta + O(\Delta\theta^2) \qquad (2.39)$$

or

$$f(U_j^{n+1}) = f(U_j^{n}) + \frac{\partial f(U_j^n)}{\partial U_j^n}\frac{\partial U_j^n}{\partial \theta}\Delta\theta + O(\Delta\theta^2) \qquad (2.40)$$

where the truncation error is of second order. To increase the order of accuracy, the following expansion is carried out;

According to the Taylor-series expansion,

$$f(\theta + \Delta\theta) = f(\theta) + f'(\theta)\,\Delta\theta + \frac{1}{2} f''(\theta)\Delta\theta^2 + O(\Delta\theta^3) \qquad (2.41)$$

$$f(\theta - \Delta\theta) = f(\theta) - f'(\theta)\,\Delta\theta + \frac{1}{2} f''(\theta)\Delta\theta^2 - O(\Delta\theta^3) \qquad (2.42)$$

Subtracting the latter from the former gives

$$f(\theta + \Delta\theta) = f(\theta - \Delta\theta) + 2f'(\theta)\,\Delta\theta + O(\Delta\theta^3) \qquad (2.43)$$

or

$$f(U_j^{n+1}) = f(U_j^{n-1}) + 2\frac{\partial f(U_j^n)}{\partial U_j^n}\frac{\partial U_j^n}{\partial \theta}\Delta\theta + O(\Delta\theta^3) \qquad (2.44)$$

Note that this equation involves two time levels, n and n-1; thus, it is termed as the two-step Taylor-series expansion (or two-step expansion in short). In equation (2.44), both $\partial f(U_j^n)/\partial U_j^n$ and $\partial U_j^n/\partial\theta$ are evaluated at time level n. $\partial f(U_j^n)/\partial U_j^n$ can be calculated analytically, and $\partial U_j^n/\partial\theta$ can be obtained through the following finite difference approximation;

$$\frac{\partial U_j^n}{\partial\theta} = \frac{1}{Pe}\left(\frac{U_{j+1}^n - 2U_j^n + U_{j-1}^n}{\Delta X^2}\right) - \frac{3U_j^n - 4U_{j-1}^n + U_{j-2}^n}{2\Delta X} + f(U_j^n) + O(\Delta X^2) \qquad (2.45)$$

Consequently, all the terms on the right-hand side can be evaluated at time level other than n+1. Substitution of equation (2.44) into equation (2.38) leads to a tridiagonal system. It is worth mentioning that the two-step expansion of $f(U_j^{n+1})$ introduces two truncation errors. One is due to the expansion in equation (2.44) and the order of error is $O(\Delta\theta^3)$; the other is due to the finite difference approximation of $\partial U_j^n/\partial\theta$ in equation (2.45) and the order of error is $O(\Delta X^2\Delta\theta)$. since both truncation errors are of third order, the accuracy of the two-step expansion is of third order, which is one order higher than that of the TPB method. Therefore, the two-step expansion can be applied to linearize the finite difference equation, equation (2.38), without additional loss of accuracy.

2.2.2 Uncoupling PDE's with Coupled Nonlinear Reaction Terms.

The two-step expansion can also be applied to a system of mixed PDE's with coupled nonlinear reaction terms, which can be represented as follows:

$$\frac{\partial U_i}{\partial \theta} = \frac{1}{Pe}\frac{\partial^2 U_i}{\partial X^2} - \frac{\partial U_i}{\partial X} + f_i(\bar{U}) , \quad i = 1, 2, \ldots, m \tag{2.46}$$

where $\bar{U} = (U_1, U_2, \ldots, U_m)^t$ and m is the number of PDE's. The finite difference expression of equation (2.46) can be written in the same form as equations (2.38), i.e.,

$$\begin{aligned}(-r_1 - 2r_2)(U_i)_{j-1}^{n+1} + (3 + 2r_1 + 2r_2)(U_i)_j^{n+1} - r_1(U_i)_{j+1}^{n+1} \\ = -r_2(U_i)_{j-2}^{n} + 2r_2(U_i)_{j-1}^{n} + (4 - r_2)(U_i)_j^{n} \\ - (U_i)_j^{n-1} + 2\Delta\theta\, f_i(\bar{U}_j^{n+1}),\end{aligned}$$

$$2 \leq j \leq N-1, \quad 1 \leq i \leq m \tag{2.47}$$

where $f_i(\bar{U}_j^{n+1})$ can be expressed in terms of the following two-step expansion;

$$f_i(\bar{U}_j^{n+1}) = f_i(\bar{U}_j^{n-1}) + \left(\sum_{k=1}^{m} \frac{\partial f_i(\bar{U}_j^n)}{\partial (U_k)_j^n}\frac{\partial (U_k)_j^n}{\partial \theta}\right) 2\Delta\theta \tag{2.48}$$

In this equation, $\partial f_i(\bar{U}_j^n)/\partial (U_k)_j^n$ can be obtained analytically from the given $f_i(\bar{U})$, and $\partial (U_k)_j^n/\partial\theta$ can be evaluated in the same way as equation (2.45). Since $f_i(\bar{U}_j^{n+1})$ is evaluated at the time levels of n and n - 1, equation (2.47) can be solved with the tridiagonal matrix method.

2.2.3 Uncoupling PDE's Coupled with ODE's and/or Algebraic Equations

The two-step expansion technique can be extended to a system of mixed PDE's coupled with ordinary differential equations (ODE's) and/or algebraic equations. For simplicity, it is assumed that the mixed PDE's given in equation (2.46) are coupled with one ODE and one algebraic equation; they are expressed as

$$\frac{\partial U_{m+1}}{\partial \theta} = g_1(\bar{U}) \tag{2.49}$$

$$h_1(\bar{U}) = 0 \tag{2.50}$$

where $\bar{U} = (U_1, U_2, \ldots, U_{m+2})^t$ and m is the number of PDE's. The first step for solving this system of equations is to solve the PDE's by the finite difference equation given in equation (2.47). $f_i(\bar{U}_j^{n+1})$ in equation (2.47) can be expressed as

$$f_i(\bar{U}_j^{n+1}) = f_i(\bar{U}_j^{n-1}) + \left(\sum_{k=1}^{m\pm2} \frac{\partial f_i(\bar{U}_j^n)}{\partial (U_k)_j^n} \frac{\partial (U_k)_j^n}{\partial \theta}\right) 2\Delta\theta \tag{2.51}$$

$$i = 1, 2, \ldots, m$$

where $\partial(U_{m+1})_j^n/\partial\theta$ is equal to $g_1(\bar{U}_j^n)$ in equation (2.49) and $\partial(U_{m+2})_j^n/\partial\theta$ can be obtained by taking the derivative of equation (2.50) with respect to θ, i.e.,

$$\frac{\partial h_1(\bar{U}_j^n)}{\partial \theta} = \sum_{k=1}^{m\pm2} \frac{\partial h_1(\bar{U}_j^n)}{\partial (U_k)_j^n} \frac{\partial (U_k)_j^n}{\partial \theta} = 0 \tag{2.52}$$

In this equation, $\partial(U_{m+2})_j^n/\partial\theta$ is the only unknown and can be readily solved. With $\partial(U_{m+1})_j^n/\partial\theta$ and $\partial(U_{m+2})_j^n/\partial\theta$ available,

$f_i(\bar{U}_j^{n+1})$ can be calculated from equation (2.51); equation (2.46) can then be solved for U_i, i=1, 2, ..., m. The second step is to solve the ODE in equation (2.49) for $(U_{m+1})_j^{n+1}$; finally, equation (2.50) is solved for $(U_{m+2})_j^{n+1}$. The same procedure can be followed if the number of ODE's or the number of algebraic equations is greater than one.

2.2.4 Example

To test the TPB method for a system of mixed PDE's with nonlinear reaction terms, the following example provides a comparison of the numerical solution obtained by the TPB method with the available analytical solution.

A system of mixed PDE's is given as:

$$\frac{\partial U_1}{\partial \theta} = \frac{1}{Pe}\frac{\partial^2 U_1}{\partial X^2} - \frac{\partial U_1}{\partial X} + 2U_2^{0.5} - \left(\frac{1}{Pe} + 1\right)U_1 \qquad (2.53)$$

$$\frac{\partial U_2}{\partial \theta} = \frac{1}{Pe}\frac{\partial^2 U_2}{\partial X^2} - \frac{\partial U_2}{\partial X} + 2\frac{U_2^{1.5}}{U_1} - \left(\frac{4}{Pe} + 2\right)U_2 \qquad (2.54)$$

$$\frac{\partial U_3}{\partial \theta} = \frac{1}{Pe}\frac{\partial^2 U_3}{\partial X^2} - \frac{\partial U_3}{\partial X} + 3\frac{U_2^{2}}{U_1} - \left(\frac{9}{Pe} + 3\right)U_3 \qquad (2.55)$$

The initial and boundary conditions for the above equations are:

$$\theta = 0, \quad U_1(0,x) = e^{-x} \qquad (2.56)$$

$$U_2(0,x) = e^{-2x} \qquad (2.57)$$

$$U_3(0,x) = e^{-3x} \qquad (2.58)$$

$$x = 0, \quad U_1(\theta,0) = (1+\theta)^2 \qquad (2.59)$$

$$U_2(\theta,0) = (1+\theta)^2 \qquad (2.60)$$

$$U_3(\theta,0) = (1+\theta)^3 \tag{2.61}$$

$$x = 1, \quad U_1(\theta,1) = (1+\theta)^2 e^{-1} \tag{2.62}$$

$$U_2(\theta,1) = (1+\theta)^2 e^{-2} \tag{2.63}$$

$$U_3(\theta,1) = (1+\theta)^3 e^{-3} \tag{2.64}$$

The numerical solution of equations (2.53) through (2.55) obtained by the present method is compared to its analytical solution given below.

$$U_1(\theta,x) = (1 + \theta)^2 e^{-x} \tag{2.65}$$

$$U_2(\theta,x) = (1 + \theta)^2 e^{-2x} \tag{2.66}$$

$$U_3(\theta,x) = (1 + \theta)^3 e^{-3x} \tag{2.67}$$

It is shown in Table 2.1 that the numerical solution is highly accurate.

2.3 CONCLUDING REMARKS

The three-point backward (TPB) finite difference method has been developed for solving mixed hyperbolic-parabolic (convection-diffusion) PDE's. For a mixed PDE with a linear reaction term, the present method resorts to the three-point backward differencing to approximate the first-order temporal and spatial derivatives, and the temporal and spatial accuracy is of second order. Moreover, the resultant finite difference equations are solved with the tridiagonal matrix method at each time step. The results of calculation have demonstrated that the TPB method substantially reduces

the numerical oscillations and diffusion; moreover, it is computationally efficient.

For a system of mixed PDE's with coupled nonlinear reaction terms, a two-step expansion technique has been derived to linearize the finite difference equations and uncouple the PDE's. The accuracy of the two-step expansion technique is of third order. The results of calculation have shown this technique can be applied to a coupled system without additional loss of accuracy. Moreover, the present method can be effectively extended to a system of mixed PDE's coupled with ODE's and/or algebraic equations.

REFERENCES

Allen, M.B. III, I. Herrera and G.F. Pinder, Numerical Modeling in Science and Engineering, pp. 201-216, Wiley, New York, 1988.

Davis, M.E., Numerical Methods & Modeling for Chemical Engineers, pp. 140-142, Wiley, New York, 1984.

Finlayson, B.A., Nonlinear Analysis in Chemical Engineering, pp. 231-265, McGraw-Hill, New York, 1980.

Khanna, R. and J. H. Seinfeld, "Mathematical Modeling of Packed Bed Reactors: Numerical Solutions and Control Model Development," in Advances in Chemical Engineering, Vol.13, J. Wei, Eds.,pp. 113-191 Academic Press, New York (1987).

Lapidus, L. and G. Pinder, Numerical Solution of Partial Differential Equations in Science and Engineering, pp. 577-580, Wiley, New York, 1982.

Oran, E.S. and J.P. Boris, Numerical Simulation of Reactive Flow, pp. 79-133, Elsevier, New York, 1987.

Smith, G.D., Numerical Solution of Partial Differential Equations: Finite Difference Methods, 3rd Ed., pp. 19-202, Clarendon Press. Oxford, 1985.

Warming, R.F. and R.M. Beam, "On the Construction and Application of Implicit Factored Scheme For Conservation Laws," SIAM-AMS Proceedings, Vol. 11, pp. 85-129 (1978).

Wen, C.Y. and L.T. Fan, Models for Flow Systems and Chemical Reactors, Marcel Dekker, New York, 1975.

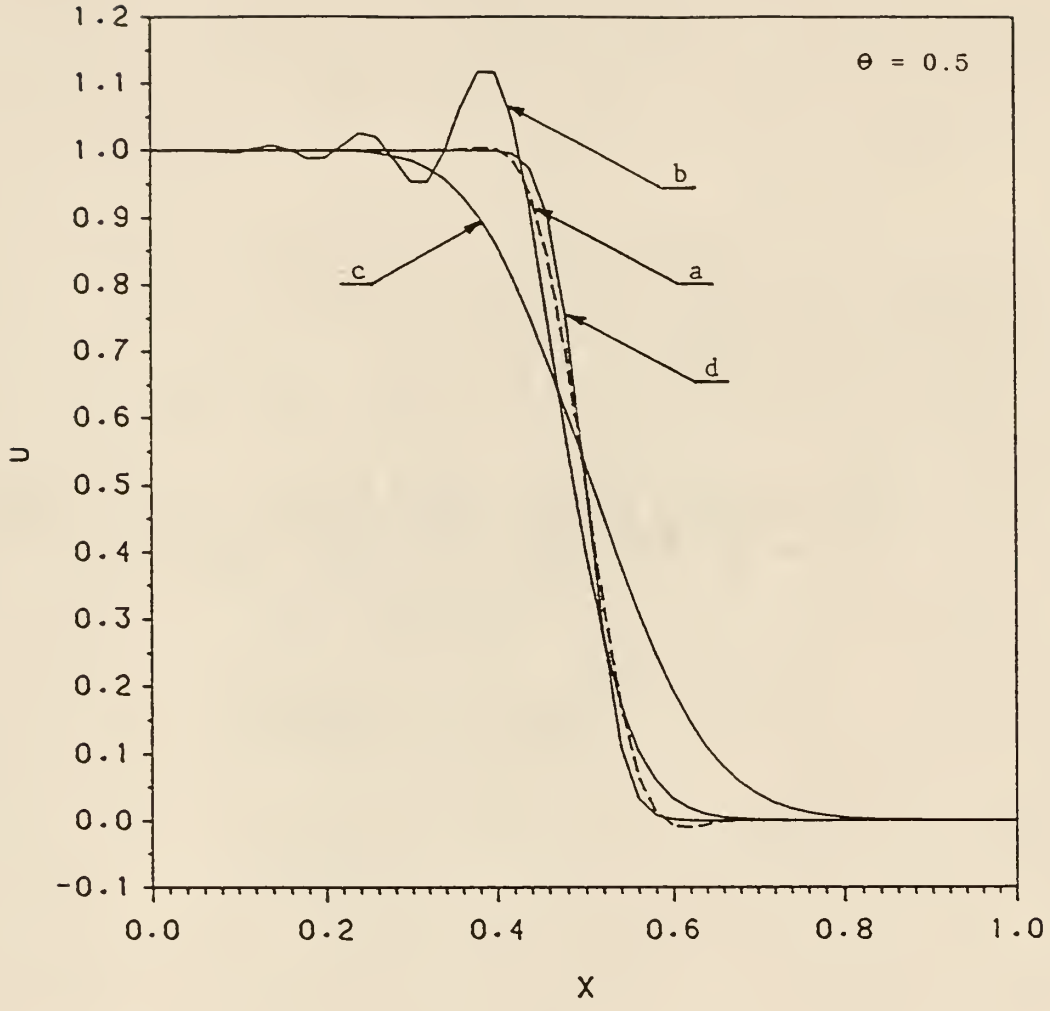

Figure 2.1. Finite difference solutions for the example:
a. TPB method ($\Delta X=0.02$, $\Delta\theta=0.01$)
b. Euler method with the central differencing ($\Delta X=0.02$, $\Delta\theta=0.0005$)
c. Euler method with the upstream differencing ($\Delta X=0.02$, $\Delta\theta=0.0005$)
d. Exact solution.

Table 2.1. Comparison between the Numerical and Analytical Solution of a System of Mixed PDE's With Coupled Nonlinear Reaction Terms

X	θ	r_1^*	r_2	r_3
0.10	5.00	0.0003	0.0012	0.0026
0.20	5.00	0.0003	0.0011	0.0022
0.30	5.00	0.0003	0.0010	0.0018
0.40	5.00	0.0003	0.0009	0.0014
0.50	5.00	0.0003	0.0008	0.0011
0.60	5.00	0.0003	0.0006	0.0007
0.70	5.00	0.0003	0.0005	0.0003
0.80	5.00	0.0002	0.0004	0.0000
0.90	5.00	0.0002	0.0003	-0.0004

* $\Delta X = 0.025$, $\Delta\theta = 0.025$

$r_i = (U_{i,TPB} - U_{i,analy})/ U_{i,analy}$

CHAPTER 3

MODELING AND NUMERICAL SIMULATION OF IN SITU NEUTRALIZATION PROCESSES

Soil neutralization is an important in situ treatment technology that is used for the cleanup of acid sludge as well as the improvement of pH of soil. In this chemical treatment, a solution of base is allowed to flow into the soil to neutralize the deposited acid. Since the transport process and chemical reactions involved in the treatment are complicated and the cost for neutralization is relatively high, it is desirable that mathematical models be developed to optimize the design of the treatment system.

Mathematical models for the movement of solute through the soil media have been reported by numerous researchers (Jury et al., 1983; Robert et al., 1985; Valocchi, 1985; Nielsen et al. 1986; Short, 1986; Grenney et al., 1987). These works have concentrated on the fate of chemicals in the subsurface environment. In contrast, the mathematical models for in situ chemical treatment processes have seldom been studied (Kosson et al., 1987; Wu et al., 1988). In these processes, contaminants deposited in soils are eliminated with chemical agents by means of chemical reactions. As a result, the models need consider not only

the transport and reaction of contaminants, but also those of chemical agents.

In the present work, in situ neutralization is modeled as a typical nonequilibrium adsorption/desorption system. The mechanism of neutralization, which is substantially different from that of ion exchange, is discussed. The model equations have been nondimensionalized, and then, dimensional analysis and numerical simulations have been conducted to determine the effects of different dimensionless model parameters on the performance of the treatment systems; such information is useful for the design of the system.

3.1 MECHANISMS OF SOIL NEUTRALIZATION

Soil neutralization can be applied to either acidic soil or basic soil. In practice, the neutralization of acidic soil is more important. To understand the mechanism of neutralization of acidic soil, it is useful to know how acidic soil forms. According to ion exchange theory, acid soil is formed by exchanging metal ions originally existing in soil with hydrogen ions. Consequently, hydrogen-saturated soil and clay are formed. However, hydrogen-saturated minerals are highly unstable. Coleman and Craig (1961) have reported that hydrogen-saturated soil and clay prepared by

strong-acid leaching or dialysis decompose rapidly to aluminum- and iron-saturated materials. The halflife for the temperature-dependent decomposition is only a few hours for many minerals. The resultant polymers of hydroxy-Al and hydroxy-Fe can be held between the lattices of expanding soil minerals. According to Bohn (1979), the mechanism of the neutralization of acidic soil can be represented as neutralization reactions of the polymers on the surfaces of soil particles. Since the neutralization reaction is very fast, the interphase transport of base from the bulk liquid to the surface of soil particles is considered as the rate limiting step of the process.

3.2 MODEL DESCRIPTION AND EQUATIONS

The entire mass of acid sludge to be neutralized can be visualized as a fixed bed. The bulk liquid is defined as the liquid phase and the soil particles are defined as the solid phase. The components involved are acid and base. One dimensional flow is assumed to prevail in the liquid phase. This gives rise to the following equation describing the effects of convection, axial dispersion, and interphase mass transfer.

$$\frac{\partial C_b}{\partial t} = E\frac{\partial^2 C_b}{\partial x^2} - v\frac{\partial C_b}{\partial x} - \frac{1}{\epsilon}k_b a(C_b - C_b^*) \qquad (3.1)$$

It is worth noting that the acid transfer rate from the solid phase to the liquid phase is very small, and its effect can be included in the base transfer term. In the convection term, v is the vertical pore velocity of solution. It is assumed to be constant and related to the superficial velocity, v_f, by

$$v = \frac{v_f}{\epsilon} \tag{3.2}$$

We are concerned with the fate of acid as well as the possible accumulation of base in it. If Z is the number of hydroxyl ions in a base molecule, we have

$$\frac{\partial q_a}{\partial t} = - \frac{Z k_b a}{\rho} (C_b - C_b^*), \qquad q_a > 0 \tag{3.3}$$

$$\frac{\partial q_b}{\partial t} = \frac{k_b a}{\rho} (C_b - C_b^*), \qquad q_a = 0 \tag{3.4}$$

The initial conditions for equations (3.1), (3.3) and (3.4) are, respectively,

$$\text{at } t = 0, \quad C_b(0,x) = 0 \tag{3.5}$$

$$q_a(0,x) = q_{ao} \tag{3.6}$$

$$q_b(0,x) = 0 \tag{3.7}$$

The boundary conditions for equation (3.1) are (Wen and Fan, 1975)

$$\text{at } x = 0, \quad vC_{bo} = v(C_b)_{o+} - E\left(\frac{\partial C_b}{\partial x}\right)_{o+} \tag{3.8}$$

$$\text{at } x = L, \quad \frac{\partial C_b}{\partial x} = 0 \tag{3.9}$$

3.3 ADSORPTION/DESORPTION RELATIONS

In equation (3.1), the interphase mass transport is related to C_b^*, the concentration of base in the solution which would be in equilibrium with that in the solid phase. Available experimental data indicate that when acidic soil is mixed with basic solution, the solution will be acidic if the resultant soil is acidic upon establishment of the adsorption/desorption equilibrium. In other words, no basic solution remains, which would be in equilibrium with the acidic soil. For those locations where q_a is equal to zero, base will be adsorbed on soil surfaces and a linear sorption equilibrium isotherm can be assumed. Thus,

$$\text{if } q_a > 0, \quad C_b^* = 0 \tag{3.10}$$

and

$$\text{if } q_a = 0, \quad C_b^* = \frac{q_b}{K_p} \tag{3.11}$$

In equations (3.10) and (3.11), only the interphase transport is considered; the mass transfer rate does not depend on the concentration of acid in the solid phase. This is not the case if the transport process is further analyzed in terms of the double layer theory (Iwata et al., 1988). This theory portrays the surface of soil particles at a low pH as positively charged, and the mass transfer rate of hydroxyl ions as proportional to the charge density, which,

in turn, is related to the pH in the soil. If the mass flux induced by electric potential is expressed in linear form, we have

$$J' = k_a(q_a - q_a^*) \tag{3.12}$$

Here q_a^* is the acid concentration where pH is equal to the isoelectric point so that the ion velocity is zero.

Since the double layer and interphase transport overlay each other, the two processes are in parallel instead of in series. Thus, the overall mass transfer will be

$$J = k_b(C_b - C_b^*) + k_a(q_a - q_a^*) \tag{3.13}$$

If q_a^* is very small and C_b^* is equal to zero, equation (3.13) can be simplified to

$$J = k_b(C_b - C_b^{**}) \tag{3.14}$$

where

$$C_b^{**} = - \frac{k_a}{k_b} q_a \tag{3.15}$$

Generally, k_a need be determined experimentally. For simplicity, it is assumed that

$$k_b >> k_a$$

in this work. In other words, the effect of double layer on the rate of mass transfer is assumed to be negligibly small, and thus, C_b^{**} approaches zero.

3.4 DIMENSIONLESS FORM OF GOVERNING EQUATIONS OF THE MODEL

To better understand the effects of the various parameters of the model on the solution and to better analyze the performance of different numerical methods, it is desirable to rewrite equations (3.1), (3.3) and (3.4) and the initial and boundary conditions, equations (3.5) through (3.9), in dimensionless form. For this purpose, the following dimensionless variables are defined;

$$\theta = \frac{tv}{L} \tag{3.16}$$

$$X = \frac{x}{L} \tag{3.17}$$

$$\bar{C}_b = \frac{C_b}{C_{bo}} \tag{3.18}$$

$$\bar{q}_a = \frac{q_a}{q_{ao}} \tag{3.19}$$

$$\bar{q}_b = \frac{\rho q_b}{\epsilon C_{bo}} \tag{3.20}$$

After substituting these definitions into equations (3.1) through (3.9), we obtain

$$\frac{\partial \bar{C}_b}{\partial \theta} = \left(\frac{E}{vL}\right)\frac{\partial^2 \bar{C}_b}{\partial X^2} - \frac{\partial \bar{C}_b}{\partial X} - \left(\frac{k_b aL}{\epsilon v}\right)\left(\bar{C}_b - \frac{\bar{q}_b}{\rho K_p/\epsilon}\right) \tag{3.21}$$

$$\frac{\partial \bar{q}_a}{\partial \theta} = -\left(\frac{k_b aL}{\epsilon v}\right)\left(\frac{\epsilon C_{bo}}{\rho q_{ao}}\right)\bar{C}_b Z \ , \qquad \bar{q}_a > 0 \tag{3.22}$$

$$\frac{\partial \bar{q}_b}{\partial \theta} = \left(\frac{k_b aL}{\epsilon v}\right)\left(\bar{C}_b - \frac{\bar{q}_b}{\rho K_p/\epsilon}\right) \ , \qquad \bar{q}_a = 0 \tag{3.23}$$

Note that E/vL is the reciprocal of the Peclet number and $k_b aL/\epsilon v$ is the Stanton number for interphase mass transfer.

Also note that the Stanton number may have different forms for different mass transfer expressions. The other two dimensionless groups can be defined as follows:

$$R_o = \frac{\epsilon C_{bo}}{\rho q_{ao}} \tag{3.24}$$

$$\bar{K}_p = \frac{\rho K_p}{\epsilon} \tag{3.25}$$

$\bar{K}_p$ in the above expression can be regarded as the dimensionless linear isotherm partition coefficient since this expression can be rewritten as

$$\bar{K}_p = \frac{\bar{q}_b}{\bar{C}_b} \tag{3.26}$$

By substituting equations (3.24) and (3.25) as well as the definitions of Peclet number and Stanton number into equations (3.21) through (3.23), we obtain, respectively,

$$\frac{\partial \bar{C}_b}{\partial \theta} = \frac{1}{Pe} \frac{\partial^2 \bar{C}_b}{\partial X^2} - \frac{\partial \bar{C}_b}{\partial X} - St_m(\bar{C}_b - \frac{\bar{q}_b}{\bar{K}_p}) \tag{3.27}$$

$$\frac{\partial \bar{q}_a}{\partial \theta} = - St_m R_o \bar{C}_b Z, \qquad \bar{q}_a > 0 \tag{3.28}$$

$$\frac{\partial \bar{q}_b}{\partial \theta} = St_m(\bar{C}_b - \frac{\bar{q}_b}{\bar{K}_p}), \qquad \bar{q}_a = 0 \tag{3.29}$$

The corresponding initial conditions are

$$\text{at } \theta = 0, \quad \bar{C}_b(0,X) = 0 \tag{3.30}$$

$$\bar{q}_a(0,X) = 1 \tag{3.31}$$

$$\bar{q}_b(0,X) = 0 \tag{3.32}$$

The corresponding boundary conditions are

$$\text{at } X = 0, \quad 1 = \left(\bar{C}_b - \frac{1}{Pe}\frac{\partial \bar{C}_b}{\partial X}\right)_{o+} \tag{3.33}$$

$$\text{at } X = 1, \quad \frac{\partial \bar{C}_b}{\partial X} = 0 \tag{3.34}$$

3.5 SOLUTION ALGORITHMS

Equation (3.27) is a convection-dispersion partial differential equation (PDE) coupled with ordinary differential equations, equations (3.28) and (3.29). The three-point backward finite difference method developed in Chapter 2 has been applied to solve these equations. The detail of the numerical procedure is given below.

Application of the TPB method to equation (3.27) yields

$$\begin{aligned}
&\frac{3\bar{C}_{b,j}^{n+1} - 4\bar{C}_{b,j}^{n} + \bar{C}_{b,j}^{n-1}}{2\Delta\theta} \\
&= \frac{1}{Pe}\left(\frac{\bar{C}_{b,j+1}^{n+1} - 2\bar{C}_{b,j}^{n+1} + \bar{C}_{b,j-1}^{n+1}}{\Delta X^2}\right) \\
&\quad - \frac{(\bar{C}_{b,j}^{n+1} - \bar{C}_{b,j}^{n}) - (\bar{C}_{b,j-1}^{n+1} - \bar{C}_{b,j-1}^{n})}{\Delta X} \\
&\quad - \frac{3\bar{C}_{b,j}^{n} - 4\bar{C}_{b,j-1}^{n} + \bar{C}_{b,j-2}^{n}}{2\Delta X} - St_m\left(\bar{C}_{b,j}^{n+1} - \frac{\bar{q}_{b,j}^{n+1}}{\bar{K}_p}\right)
\end{aligned} \tag{3.35}$$

Since equation (3.27) is coupled with equation (3.29), equation (3.35) can not be solved independently. If the

second-order Runge-Kutta method is applied to equation (3.29), $\bar{q}_{b,j}^{n+1}$ can be expressed as

$$\frac{\bar{q}_b^{n+1}}{\bar{K}_p} = b_1\bar{C}_{b,j}^{n+1} + b_2\bar{C}_{b,j}^{n} + b_3\bar{q}_{b,j}^{n} \tag{3.36}$$

where

$$b_1 = \frac{\Delta\theta St_m}{2\bar{K}_p} \tag{3.37}$$

$$b_2 = \frac{\Delta\theta St_m}{2\bar{K}_p}\left(1 - \frac{\Delta\theta St_m}{\bar{K}_p}\right) \tag{3.38}$$

$$b_3 = \frac{1}{\bar{K}_p}\left(1 - \frac{\Delta\theta St_m}{\bar{K}_p} + \frac{(\Delta\theta St_m)^2}{2\bar{K}_p^2}\right) \tag{3.39}$$

Substituting equation (3.36) into equation (3.35) yields

$$\begin{aligned}&(-r_1 - 2r_2)\bar{C}_{b,j-1}^{n+1} + (3 + 2r_1 + 2r_2 + r_3 - r_3b_1)\bar{C}_{b,j}^{n+1} \\ &- r_1\bar{C}_{b,j+1}^{n+1} \\ &= (-r_2)\bar{C}_{b,j-2}^{n} + 2r_2\bar{C}_{b,j-1}^{n} + (4 - r_2 + r_3b_2)\bar{C}_{b,j}^{n} \\ &- \bar{C}_{b,j}^{n-1} + r_3b_3\bar{q}_{b,j}^{n}\end{aligned} \tag{3.40}$$

where

$$r_1 = \frac{2\Delta\theta}{Pe\Delta X^2}, \qquad r_2 = \frac{\Delta\theta}{\Delta X}, \qquad r_3 = 2\Delta\theta St_m$$

Note that a tridiagonal system is generated in equation (3.40). In each time step, equation (3.40) is solved with the tridiagonal method for $\bar{C}_{b,j}^{n+1}$, j=0,N. After $\bar{C}_{b,j}^{n+1}$ is obtained, $\bar{q}_{a,j}^{n+1}$ or $\bar{q}_{b,j}^{n+1}$ is calculated by the second-order Runge-Kutta method, which gives

$$\bar{q}_{a,j}^{n+1} = \bar{q}_{a,j}^{n} - 0.5St_m R_o Z(\bar{C}_{b,j}^{n+1} + \bar{C}_{b,j}^{n}), \quad \bar{q}_{a,j}^{n} > 0 \tag{3.41}$$

$$\bar{q}_{b,j}^{n+1} = \bar{q}_{b,j}^{n} + 0.5St_m R_o Z(\bar{C}_{b,j}^{n+1} + \bar{C}_{b,j}^{n}), \quad \bar{q}_{a,j}^{n} = 0 \tag{3.42}$$

Note that base accumulates only after acid is completely neutralized. Therefore, at any grid point, if $q_{a,j}^{n}$ is greater than zero, $q_{a,j}^{n+1}$ is calculated by equation (3.41) while $q_{b,j}^{n+1}$ remains zero. If $q_{a,j}^{n}$ is equal to zero, $q_{b,j}^{n+1}$ is calculated by equation (3.42).

3.6 RESULTS AND DISCUSSION

Equations (3.27) through (3.29) contain four dimensionless numbers, Peclet number, Stanton number, R_o and $\bar{K}_p$. The extent of axial dispersion is considered to be slight in a nonequilibrium system (Grenney, 1987); thus, Pe is fixed at 100. The effects of the remaining three parameters, St_m, R_o and $\bar{K}_p$, on the neutralization time and the accumulation of base in the solid phase are analyzed. The neutralization time, t_n, is defined as the time required to completely neutralize the acid in the solid phase, and its dimensionless form is defined as the dimensionless neutralization time, θ_n. Since the rate of neutralization varies along the soil bed, the accumulation of base in the solid phase occurs where the neutralization has already been

accomplished. This not only renders the solid phase basic, but also increases the neutralization time since the base accumulated in the solid phase becomes unavailable for neutralization.

3.6.1 Effect of St_m

By definition, St_m mainly reflects the ratio of the mass transfer coefficient to the pore velocity or the ratio of the interphase transport rate of the key component to the rate of transport of this component accompanied by the convective flow through the soil bed (or the convective transport rate in short). As a result of the interphase transport of base from the liquid phase into the soil particles, neutralization of acid and accumulation of base in the solid phase take place. Meanwhile, as a result of the convective transport, a portion of base in the feed solution moves along with bulk flow and eventually flows out of the soil bed. The larger the St_m, the faster the neutralization rate and the more extensive the accumulation of base as well as the less active the convective transport. This is demonstrated in the concentration profile of base in the solution, $\bar{C}_b$, at a fixed time but at different values of St_m in Figure 3.1. Note that when St_m is large, the interphase transport is dominant and a large portion of the base in the solution is adsorbed into the solid phase before being

convected out of the soil bed. Consequently, the change in the concentration profiles of the base in the solution, $\bar{C}_b$, is indeed steep. In contrast, when St_m is small, the convective transport is dominant, and a large portion of the base moves out of the soil bed before being adsorbed into the solid phase. Thus, the change in the concentration profile of the base in the solution is quite flat. In an extreme case of St_m being zero, no interphase mass transport occurs, and therefore, the profile of $\bar{C}_b$ remains fixed at 1.

Figures 3.2 and 3.3 show the concentration profiles of base in the solution, $\bar{C}_b$, acid in the solid phase, $\bar{q}_a$, and base in the solid phase, $\bar{q}_b$, with St_m of 2 and 20, respectively. To render $\bar{q}_b$ to be within a range from 0 to 1, $\bar{q}_b/\bar{K}_p$, instead of $\bar{q}_b$, is plotted against X. When St_m is 2, all three profiles are quite flat. However, as St_m increases to 20, these profiles become very steep, and the profile of $\bar{q}_b/\bar{K}_p$ approaches to that of $\bar{C}_b$; this can be attributed to the very fast interphase transport. Obviously, the larger the St_m, the closer the two profiles; as St_m approaches to infinity, the two profiles will merge, i.e., $\bar{q}_b = \bar{K}_p\bar{C}_b$. This indicates that an equilibrium will be established between the liquid and solid phases, and the mass transport will cease to be the rate limiting step.

In Figure 3.4, the dimensionless neutralization time, θ_n, defined as the dimensionless time required to neutralize all of the acid, is plotted against St_m at fixed R_o and $\bar{K}_p$. It indicates that as St_m increases, θ approaches asymptotically to a certain value and remains constant for $St_m > 3$. Thus, θ is mainly determined by the ratio of the concentration of base in the feed solution to the initial concentration of acid in the solid phase, R_o, and by the dimensionless linear isotherm partition coefficient, $\bar{K}_p$. In the region of $St_m < 3$, the interphase mass transport becomes the controlling step of the entire process, and therefore, St_m significantly affects θ_n. Note that the critical value of St_m, e.g., 3, in Figure 3.4, will vary with changes in R_o and $\bar{K}_p$.

3.6.2 Effect of R_o

By definition, R_o represents the ratio of the concentration of base in the feed solution to the initial concentration of acid in the soil. Comparison of Figure 3.5 with Figure 3.2 indicates that the increase in R_o from 0.05 to 0.1 does not significantly affect the concentration profile of base in the solution, $\bar{C}_b$. However, it significantly affects the concentration profile of acid in the solid phase, $\bar{q}_a$, since the rate of change of the acid concentration is proportional to R_o, as indicated in

equation (3.28). The dimensionless neutralization time, θ_n, depends upon the rate of change of the acid concentration in the solid phase; thus, the larger the R_o, the smaller the θ_n. This is plotted in Figure 3.6 with St_m as the parameter. Note that the change in R_o has a pronounced effect on θ_n when St_m is small. Under this situation, the accumulation of base in the solid phase is not appreciable, and θ_n is mainly determined by the rate of change of the acid concentration. With the increase in St_m, the rate of accumulation of base, expressed in equation (3.29), becomes increasingly important. Consequently, the effect of R_o on θ_n is reduced. It is also observed in Figure 3.5 that R_o only slightly affects the profile of $\bar{q}_b/\bar{K}_p$. Nevertheless, the actual extent of accumulation of base in the solid phase increases with R_o according to the definition of $\bar{q}_b$, equation (20).

3.6.3 Effect of $\bar{K}_p$

The dimensionless linear isotherm partition coefficient, $\bar{K}_p$, signifies the adsorption/desorption equilibrium relationship of base or the capacity of base to accumulate in the solid phase. The larger the $\bar{K}_p$, the greater the capacity of accumulation of base in the solid phase. Moreover, $\bar{K}_p$ affects the rate of accumulation of base in the solid phase. As indicated in equation (3.29), the larger the $\bar{K}_p$, the faster the rate of accumulation of base

in the solid phase. Figures 3.2 and 3.7 demonstrate that as $\bar{K}_p$ decreases from 40 to 4 and St_m remains constant, $\bar{q}_b/\bar{K}_p$ increases. But, if the corresponding $\bar{q}_b$ is calculated in both cases, $\bar{q}_b$ will decrease, which is consistent with equation (3.29). The effect of $\bar{K}_p$ on θ_n can also be divided into two regions. As observed in Figure 3.8, $\bar{K}_p$ has little effect on θ when St_m is 2. This is due to the slow rate of accumulation of base in the solid phase. In contrast, θ_n significantly increases with the increase in $\bar{K}_p$ when St_m is 20. The reason is that with the increase in $\bar{K}_p$, both the rate and capacity of base to accumulate in the solid phase increase.

3.7 CONCLUDING REMARKS

A model for simulating the in situ neutralization process has been developed, and the mechanism and equilibrium relations are discussed. The model gives rise to a convection-dispersion PDE and a set of two ODE's. The PDE has been solved with a three-point backward finite difference method. Four dimensionless numbers have been identified as the physically significant parameters. The extent of axial dispersion is considered to be slight in a nonequilibrium system; thus, Pe is fixed at 100. The

effects of the other three dimensionless numbers, St_m, R_o and $\bar{K}_p$, are summarized as follows:

a. St_m reflects mainly the ratio of the rate of interphase transport of the key component to the rate of convective transport of this component. The mass transport in the neutralization process can be divided into two regions. When St_m is greater than a critical value, the interphase transport is more dominant than the convective transport, and the accumulation of base is significant. When St_m is smaller than this critical value, both interphase transport and convective transport are appreciable, and the accumulation of base is unimportant.

b. R_o represents the ratio of the concentration of base in the feed solution to the initial concentration of acid in the solid phase. The larger the R_o, the faster the rate of change of acid concentration in the solid phase, and thus, the shorter the neutralization time. Moreover, R_o has a more pronounced effect on the neutralization time for a smaller St_m than for a larger St_m.

c. $\bar{K}_p$, signifying the capacity of base to accumulate in the solid phase, affects appreciably the dimensionless neutralization time, θ_n, only if St_m is near or greater than the critical value. In this case, the rate of the accumulation of base in the solid phase is enhanced substantially. The larger the $\bar{K}_p$, the more extensive the

accumulation of base in the solid phase, and thus, the longer the dimensionless neutralization time, θ_n.

The present model can be extended readily to any nonequilibrium in situ chemical treatment system in which a contaminant deposited in the solid phase will be eliminated with a chemical agent by means of a fast chemical reaction.

NOTATION

a = surface area of the control volume, m^2/m^3

C_b = concentration of base in the liquid phase, $kmol/m^3$

C_b^* = concentration of base in the solution which would be in equilibrium with that in the soil, $kmol/m^3$

C_b^{**} = equilibrium concentration of base which is defined by equation (3.15), $kmol/m^3$

C_{bo} = concentration of base in the feed solution, $kmol/m^3$

$\bar{C}_b$ = dimensionless concentration of base in the liquid phase, $\bar{C}_b = C_b/C_{bo}$

E = dispersion coefficient, m^2/hr

J = total mass flux of base from liquid phase to solid phase, $kg/m^2/hr$

J' = mass flux of base induced by electric potential, $kg/m^2/hr$

k_a = mass transfer coefficient of the acid due to electrical potential, kg/m^2hr

k_b = mass transfer coefficient of the base, m/hr

K_p = linear isotherm partition coefficient, m^3/kg

L = depth of the contaminated soil, m

q_a = concentration of acid in the solid phase, $kmol/kg$

q_{ao} = initial concentration of acid in the solid phase, $kmol/kg$

$\bar{q}_a$ = dimensionless concentration of acid in the solid phase, $\bar{q}_a = q_a/q_{ao}$

q_b = concentration of base in the soil, kmol/kg

$\bar{q}_b$ = dimensionless concentration of base in the soil, $\bar{q}_b = \rho q_b/\epsilon C_{bo}$

v = pore velocity of the liquid, m/hr

v_f = superficial velocity of the liquid, m/hr

t = time, hr

t_n = neutralization time, hr

x = vertical position, m

X = dimensionless vertical position, X = x/L

Z = number of hydroxyl ions in a base molecule, Z is equal to 2 in the present work.

GREEK LETTERS

ρ = bulk density of the soil, kg/m^3

ϵ = volumetric content of liquid in the control volume

θ = dimensionless time, $\theta = tv/L$

θ_n = dimensionless neutralization time, $\theta = t_n v/L$

REFERENCES

Bohn, H.L., B.L. McNeal, and G.A. O'Connor, Soil Chemistry, pp. 195-216, Wiley, New York, 1979.

Coleman, N.T. and D. Craig, "The Spontaneous Alteration of Hydrogen Clay," Soil Sci. 91,14-18 (1961).

Grenney, W.J., C.L. Caupp, R.C. Sims, and T.E. Short, " A Mathematical Model for the Fate of Hazardous Substances in Soil: Model description and Experimental Results," Hazardous Waste and Hazardous Materials, 4, 223-239 (1987).

Iwata S., T. Tabuchi, and B. P. Warkentin, Soil-Water Interaction, Mechanisms and Applications, Marcel Dekker, New York, 1988.

Jury, W. A., W. F. Spencer, and W. J. Farmer, "Behavior Assessment Model for Trace Organics in Soil: I. Model Description," J.Environ.Qual., 12, 558-564 (1983).

Kosson, D.S., G.C. Agnihotri, and R.C. Ahlert, "Modeling and Simulation of A Soil-Based Microbial Treatment Process," J. of Hazardous Materials, 14, 191-211 (1987).

Nielsen, D.R., M.T. van Genuchten, and J.W. Biggar, "Water Flow and Solute Transport Processes in the Unsaturated Zone," Water Resources Research, 22, 89S-108S (1986).

Robert, P.V., M. Reinhart, G.D. Hopkins, and R.S. Summers, "Advection-Dispersion-Sorption Models for Simulating the Transport of Organic Contaminants," in Ground Water Quality, C.H.Ward, W. Giger and P.L. McCarty, Eds., pp. 425-445, Wiley, New York, 1985.

Short, T. E., "Modeling of Processes in the Unsaturated Zone," in Land Treatment: A Hazardous Waste Management Alternative, R.C. Loehr and J.F. Malina, Jr., Eds., Water Resources Symposium No. 13, Center for Research in Water Resources, pp. 211-240. The University of Texas, Austin, TX, 1986.

Valocchi, A.J., "Validity of the Local Equilibrium Assumption for Modeling Sorbing Solute Transport through Homogeneous Soil," Water Resources Research, 21, 808-820 (1985).

Wen, C.Y. and L.T. Fan, Models for Flow Systems and Chemical Reactors, Marcel Dekker, Inc., New York, 1975.

Wu, J.C., L.T.Fan and L.E.Erickson, "Mathematical Simulation of In-Situ Neutralization and Biodegradation Processes", Proceedings of the Conference on Hazardous Waste Research, Kansas State University, Manhattan, KS (1988).

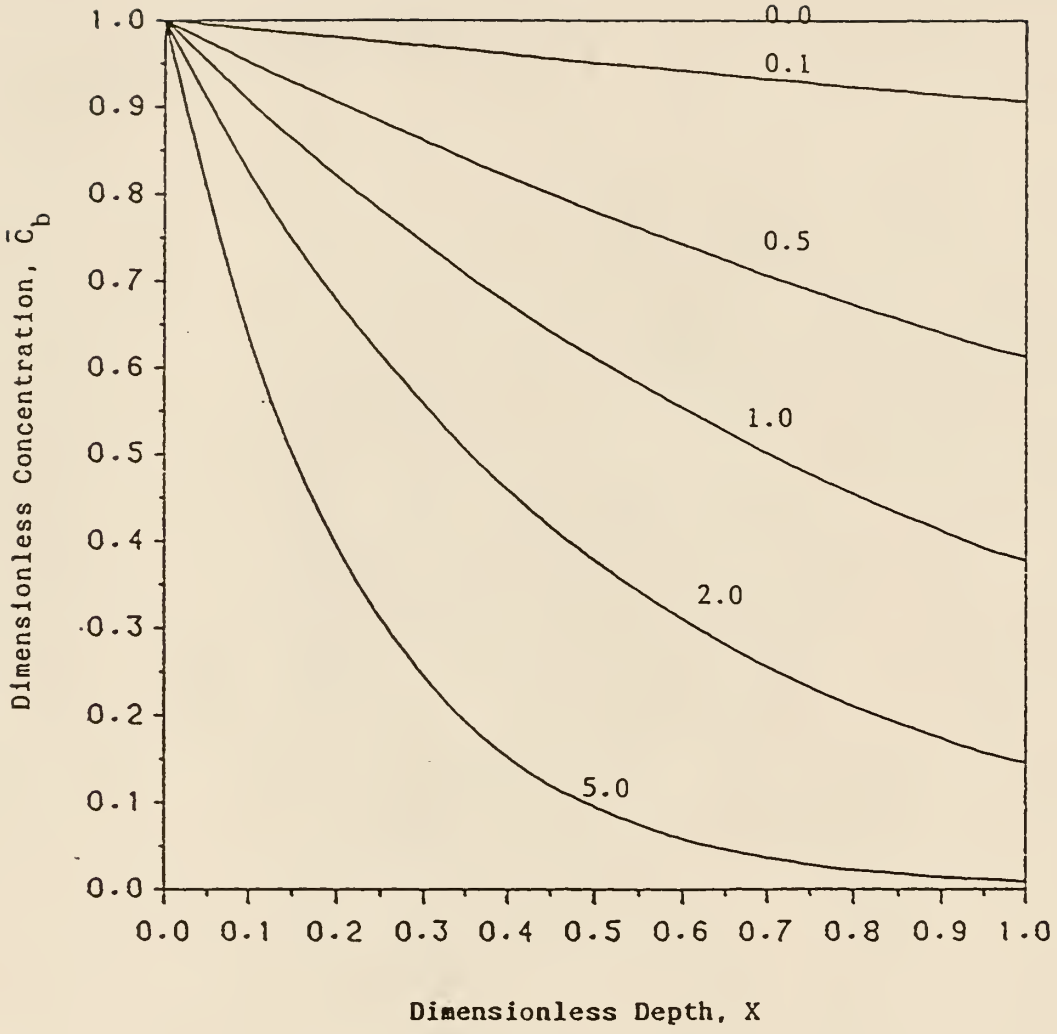

Figure 3.1. Effect of St_m on the concentration distribution of base in solution at Θ=10 with St_m as the parameter: Pe=100, R_o=0.0125 and $\bar{K}_p$=40.

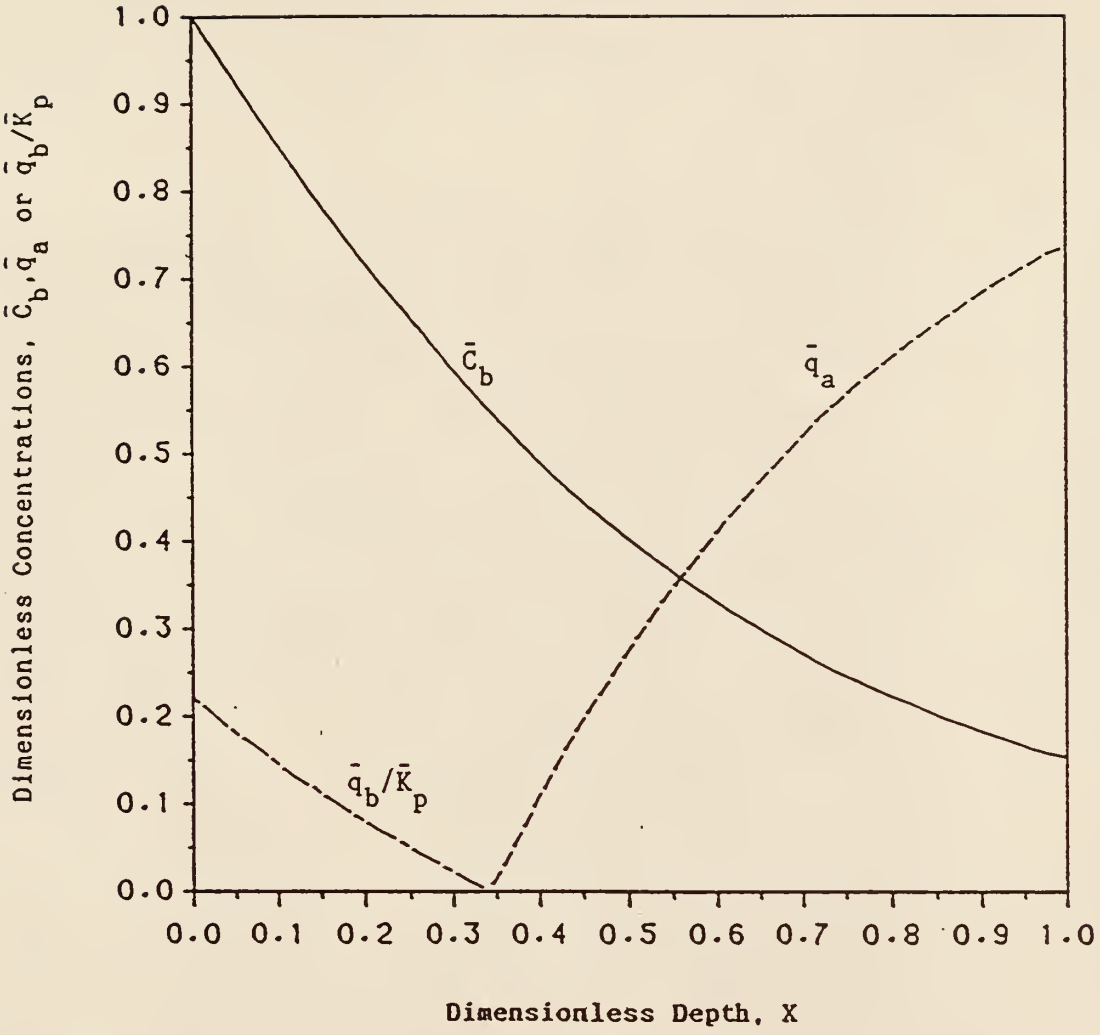

Figure 3.2. Concentration profiles of base in the solution, acid in the soil, and base in the soil at Θ=10: Pe=100, St_m=2, R_o=0.05 and $\bar{K}_p$=40.

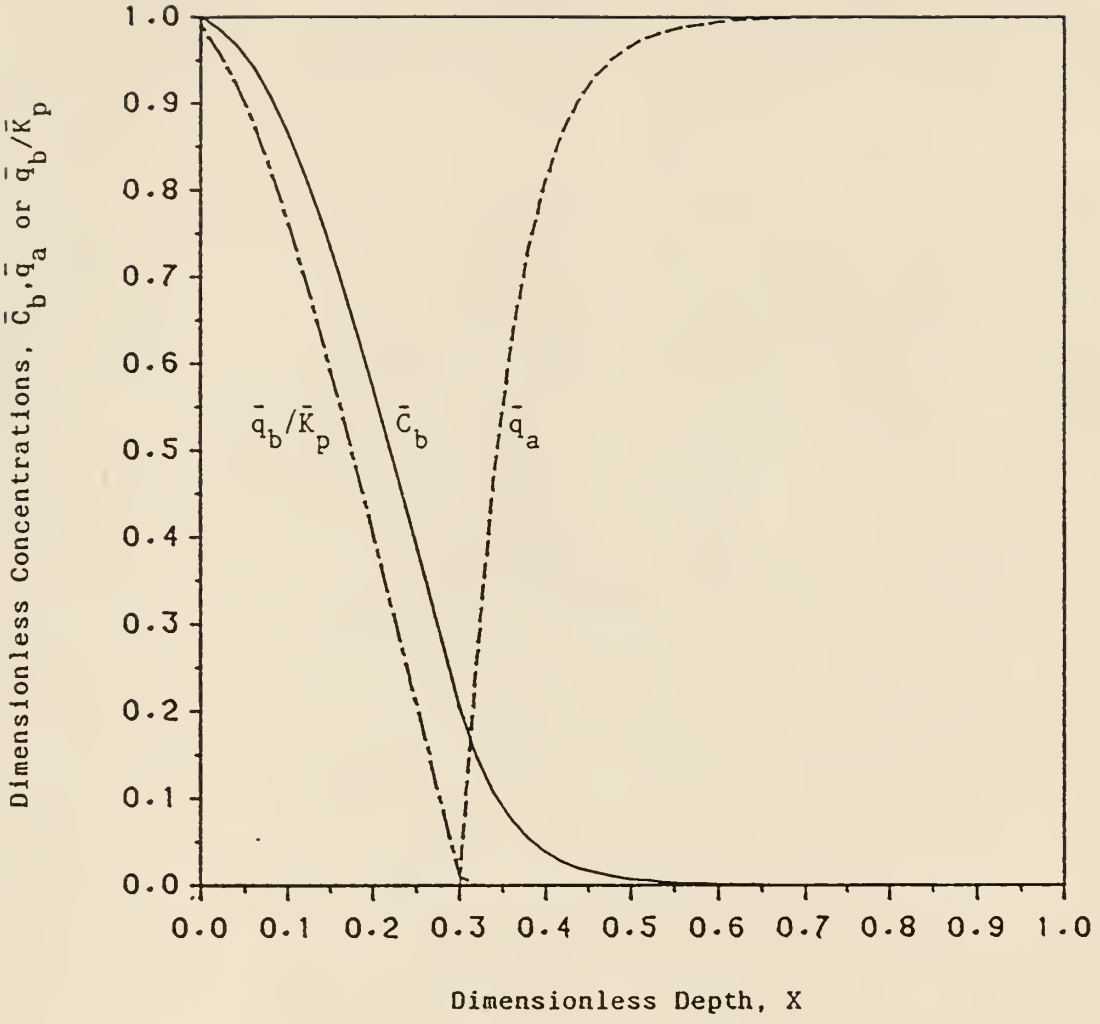

Figure 3.3. Concentration profiles of base in the solution, acid in the soil, and base in the soil at θ=10: Pe=100, St_m=20, R_o=0.05 and $\bar{K}_p$=40.

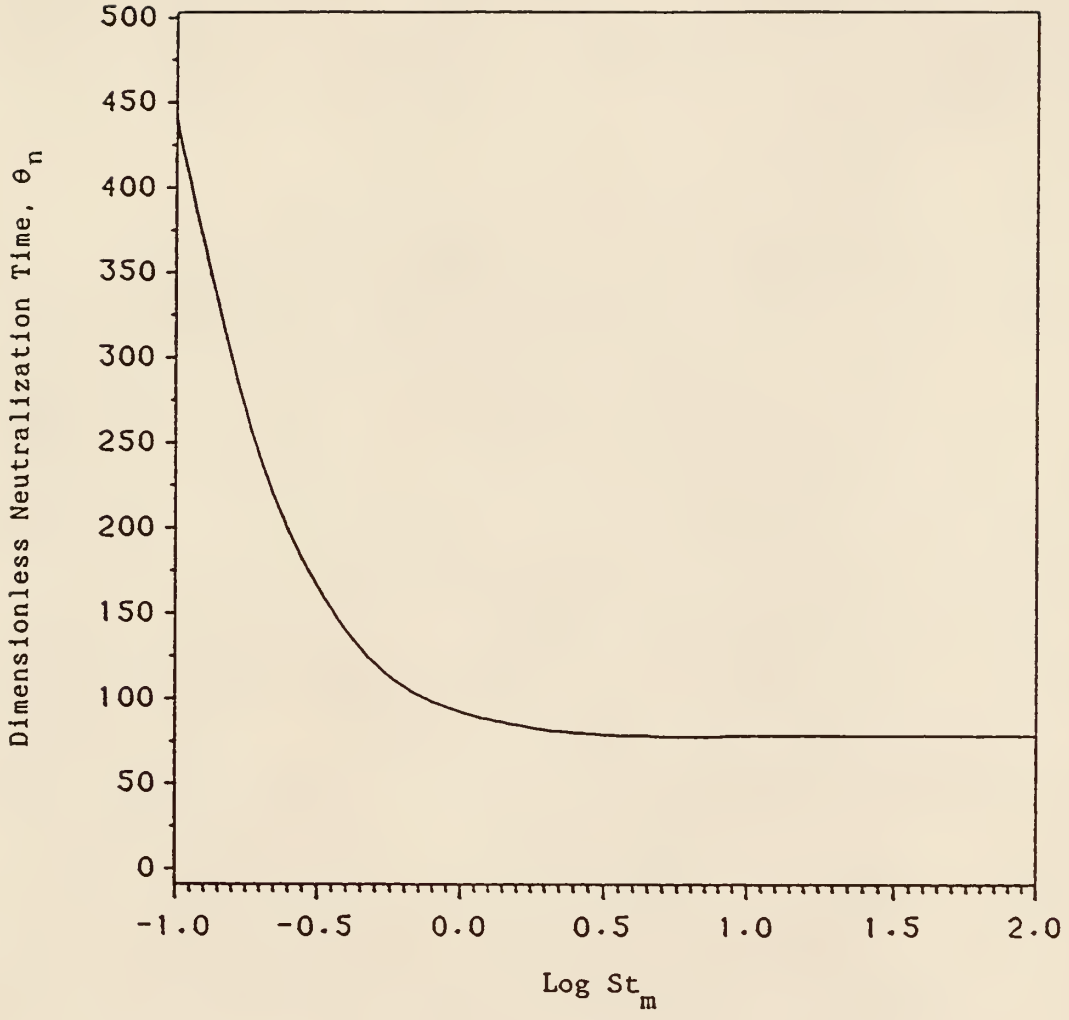

Figure 3.4. Effect of St_m on the dimensionless neutralization time: Pe=100, R_o=0,0125 and $\bar{K}_p$=40.

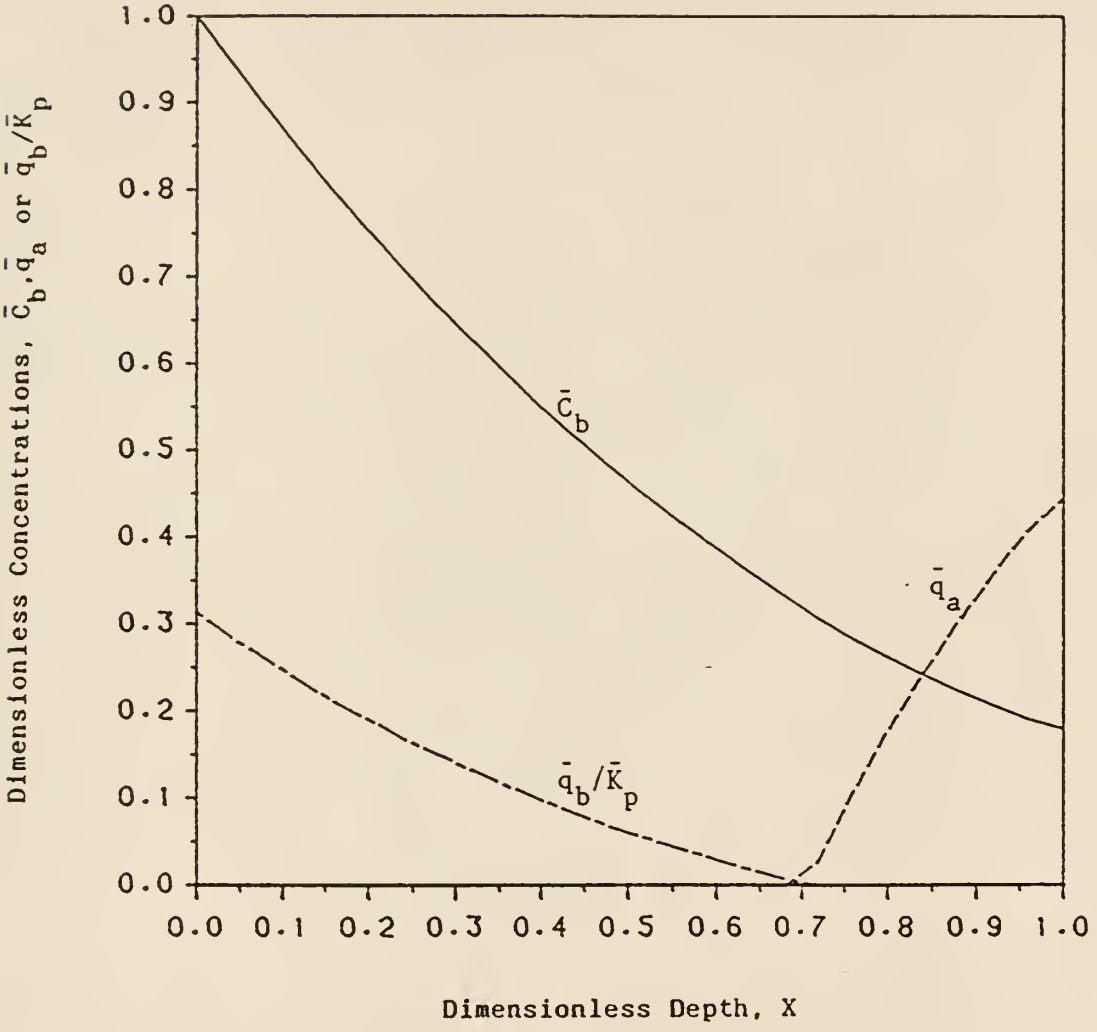

Figure 3.5. Concentration profiles of base in the solution, acid in the soil, and base in the soil at θ=10: Pe=100, St_m=2, R_o=0.1 and $\bar{K}_p$=40.

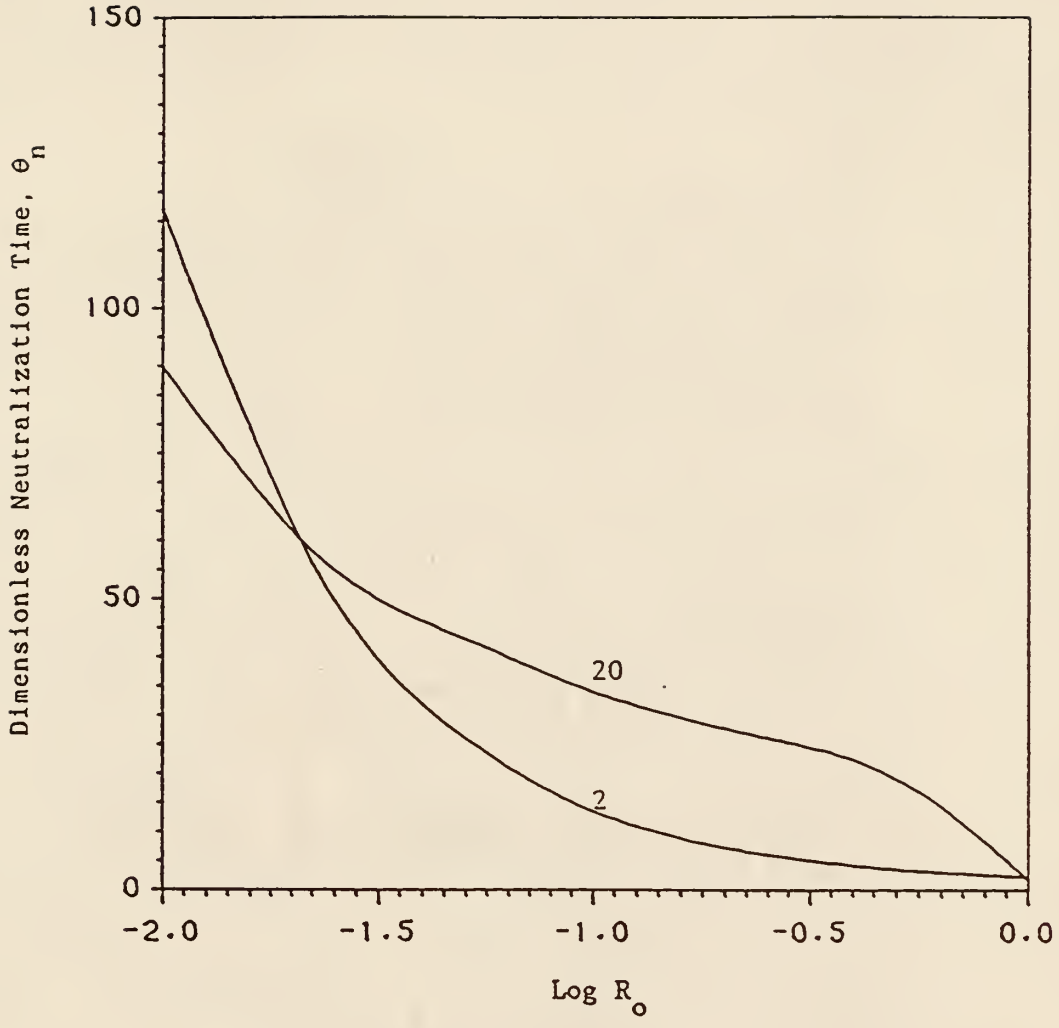

Figure 3.6. Effect of R_o on the dimensionless neutralization time with St_m as the parameter: Pe=100 and $\bar{K}_p$=40.

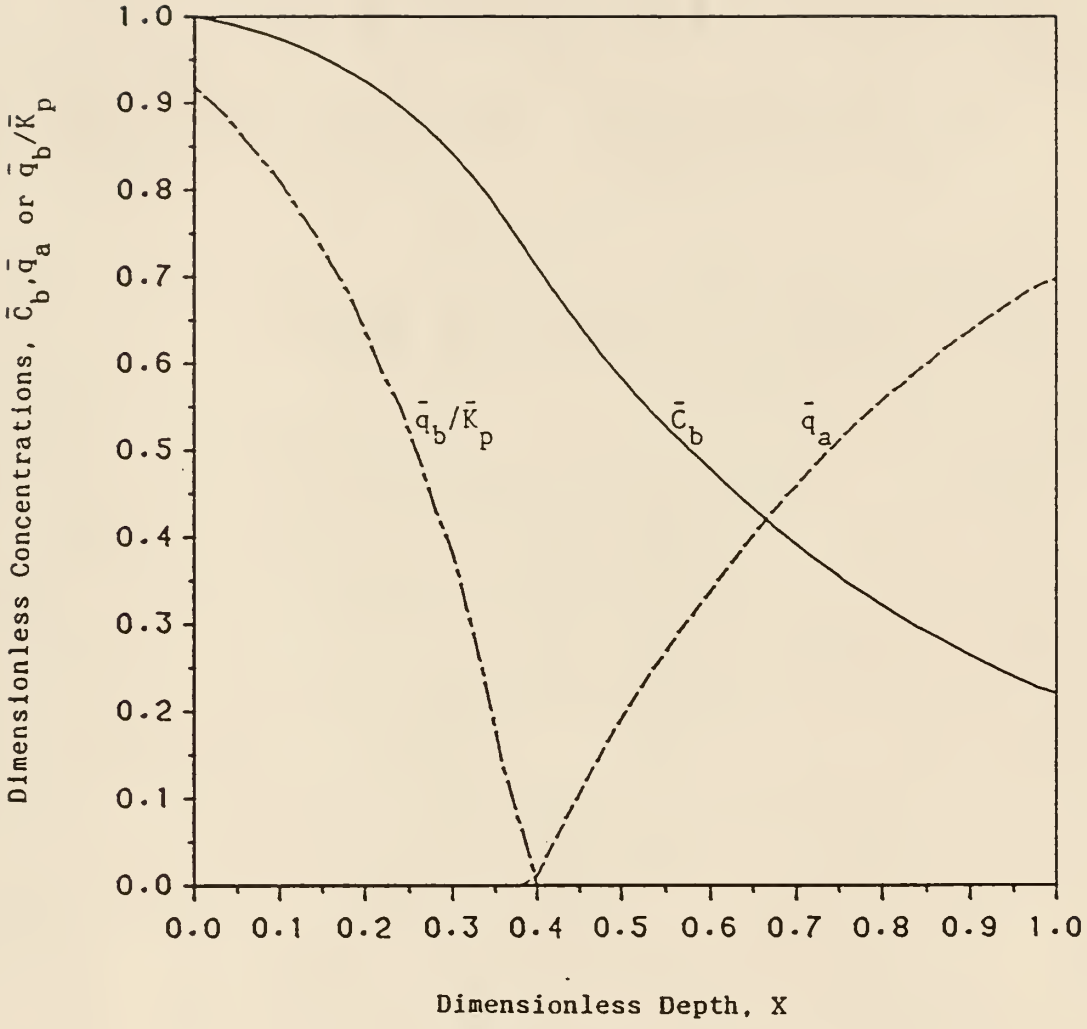

Figure 3.7. Concentration profiles of base in the solution, acid in the soil, and base in the soil at Θ=10: Pe=100, St_m=2, R_o=0.05 and $\bar{K}_p$=4.

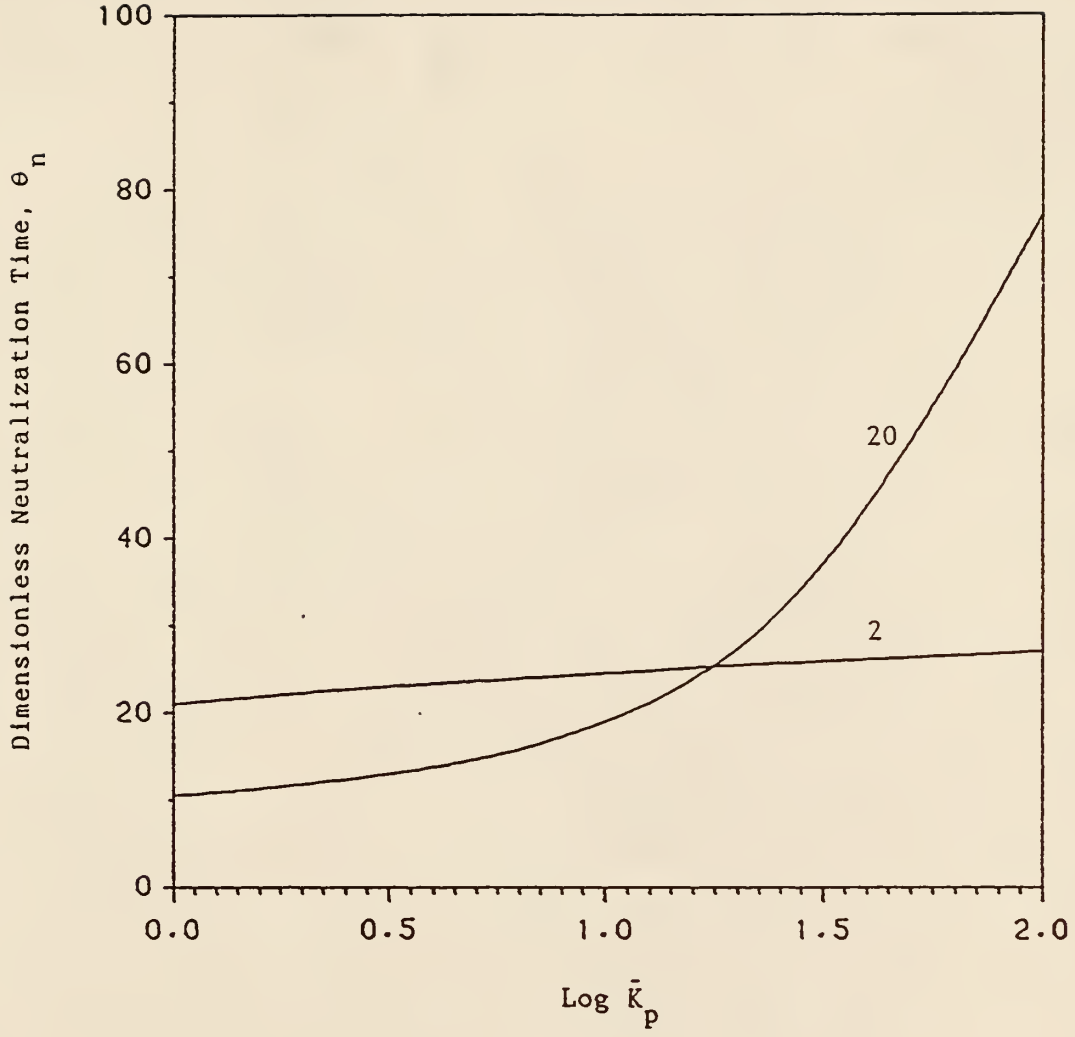

Figure 3.8. Effect of $\bar{K}_p$ on the dimensionless neutralization time with St_m as the parameter: Pe=100 and R_o=0.05.

CHAPTER 4

MODELING AND SIMULATION OF IN SITU BIOREMEDIATION PROCESSES

In situ bioremediation of contaminated soil is an innovative and cost effective treatment technology. This technology exploits the capability of naturally occurring microorganisms to decompose toxic substances deposited in a soil bed; it can be applied to the cleanup of organic sludge, where organic compounds with high molecular weights are adsorbed on the soil particles. To aerobically operate the biodegradation process, water containing oxygen is allowed to flow through the soil bed. The flow behavior of water through the soil bed is very similar to that observed in bioremediation of contaminated groundwater.

Several mathematical models have been proposed for simulating in situ bioremediation of contaminated groundwater (Bouwer and McCarty, 1984; Borden and Bedient, 1986; Molz et al., 1986; Lee et al., 1988). These models focus mainly on contaminant transport from the bulk liquid to microorganisms attached to particle surfaces (Baveye and Valocchi, 1989); the transport within the pore network is seldom studied because contaminants are mainly in the bulk liquid. Few models have been proposed for bioremediation of contaminated soil. In bioremediation of contaminants in a

soil bed, contaminants are initially adsorbed in soil particles. Consequently, the rate of biodegradation is generally controlled by transport resistance to contaminant migration within the pore network, and the transport resistance to contaminant diffusion across a stagnant layer, or immobile water, adjacent to particle surfaces becomes negligible.

In this chapter, a mathematical model has been developed for simulating bioremediation of contaminated soil. The effects of insufficient oxygen supply, growth of biomass and resistance to contaminant migration on the rate of contaminant degradation have been examined by numerically simulating the dynamic behavior of in situ biodegradation processes.

4.1 MODEL DEVELOPMENT

Organic contaminants are initially deposited in a soil bed. Water is allowed to flow through the bed continuously, thereby saturating the bed. The dissolved oxygen in the water effects aerobic biodegradation. By consuming substrate, including all contaminants, oxygen and other nutrients, naturally occurring microorganisms grow both in the solid phase as immobile microcolonies, which are clusters of microorganisms attached to the surface of soil

particles, and in the liquid phase as suspended microorganisms.

4.1.1 Assumptions

The following major assumptions are made in deriving the model equations for bioremediation of contaminated soil.

a. Water in interstices or pores of the soil bed constitutes the liquid phase and the remaining part of the bed is considered as the solid phase. No gas phase exists because the bed is saturated with water.

b. Only three components, substrate, oxygen and biomass, are involved in biodegradation.

c. Macroscopically, one dimensional flow prevails through the liquid phase. The void fraction in any cross-section of the soil bed is constant, and thus, the pore velocity of water is constant.

d. No convective flow and dispersion occur in the solid phase.

e. The microcolonies in the solid phase are attached to the surface of soil particles, i.e., the interface between the solid and liquid phases, where the supply of oxygen is more effective than the inside of soil particles.

f. The biodegradation by microcolonies takes place at the interface between the liquid and solid phases; in

other words, no reaction proceeds in the bulk of the solid phase.

g. The concentration gradients across the stagnant liquid layer, adjacent to the interface between the liquid and solid phases, are negligible, and thus, the concentrations of substrate and oxygen extracted by the microcolonies are equal to those in the bulk of the liquid. The stagnant layer is extremely thin due to the small average diameter of the macropores in soil which is generally less than 0.5 mm (Iwata et al., 1988).

h. The microcolonies cover only a portion of the interfacial area.

4.1.2 Derivation of a General Model

The schematic diagram of the transport and biodegradation in a controlled volume is given in Figure 4.1. The mass balance of component i in the liquid phase gives rise to

$$\epsilon A(\Delta x)\frac{\partial C_i}{\partial t} = \epsilon A(-E\frac{\partial C_i}{\partial x} + vC_i)\Big|_x - \epsilon A(-E\frac{\partial C_i}{\partial x} + vC_i)\Big|_{x+\Delta x} + \epsilon A(\Delta x)r_i^L - A(\Delta x)aj_i^L \quad (4.1)$$

where subscript i is s, o or b, standing for substrate, oxygen or biomass, respectively; A is the cross-sectional area; a is the interfacial area per unit volume of the bed; and ϵ is the void fraction of the bed or the volume fraction

of the bulk of the liquid phase. Dividing both sides of equation (4.1) by $A\Delta x$ and letting Δx approach to zero give

$$\epsilon\frac{\partial C_i}{\partial t} = \epsilon E\frac{\partial^2 C_i}{\partial x^2} - \epsilon v\frac{\partial C_i}{\partial x} + \epsilon r_i^L - aj_i^L \qquad (4.2)$$

The corresponding mass balance in the solid phase yields

$$\rho A(\Delta x)\frac{\partial q_i}{\partial t} = A(\Delta x)aj_i^s \qquad (4.3)$$

where ρ is the bulk density of the bed. This equation can be simplified to

$$\rho\frac{\partial q_i}{\partial t} = aj_i^s \qquad (4.4)$$

The rate of mass transfer of component i from the liquid phase to the interface must be equal to the sum of the rate of its transfer from the interface to the bulk of the solid phase and the rate of its consumption at the interface, i.e.,

$$aj_i^L = aj_i^s + \rho(-r_i^{sf}) \qquad (4.5)$$

Substituting this equation into equation (4.2) leads to

$$\epsilon\frac{\partial C_i}{\partial t} = \epsilon E\frac{\partial^2 C_i}{\partial x^2} - \epsilon v\frac{\partial C_i}{\partial x} + \epsilon r_i^L + \rho r_i^{sf} - aj_i^s \qquad (4.6)$$

Equations (4.4) and (4.6) are the general transport equations for component i in the solid and liquid phases, respectively. This set of equations gives rise to two classes of transport models, equilibrium and nonequilibrium.

If the rates of adsorption and desorption of all components are sufficiently fast so that the concentrations

in the liquid phase, C_i's, are in equilibrium with those in the solid phase, q_i's, the resultant model will be an equilibrium model. For component i in such a model, equations (4.4) and (4.6) merge naturally into a single equation through an equilibrium relation (see Appendix I). The equilibrium model is widely used in simulating in situ bioremediation of contaminated groundwater (see, e.g., Valocchi, 1985). In contrast, if the rates of adsorption and desorption of any one of the components are controlled by transport within the pore network in the solid phase so that its concentration in the liquid phase is not in equilibrium with that in the solid phase, the resultant model will be a nonequilibrium model. Separate equations, equations (4.4) and (4.6), are required for this component.

In bioremediation of contaminated soil, the substrate is initially deposited in soil particles and the rate of substrate desorption from the soil particles to the liquid phase is generally controlled by transport within their pore network; thus, the concentration of substrate in the liquid phase is not in equilibrium with that in the solid phase. Consequently, the nonequilibrium model is more appropriate than the equilibrium model for bioremediation of contaminated soil.

4.1.3 Derivation of the Nonequilibrium Model

As stated earlier, both equations (4.4) and (4.6) are required for substrate. In terms of the film model, the mass flux of the substrate, j_s^s, in these equations can be expressed as

$$(-j_s^s) = k_s'(q_s - q_s^*) \tag{4.7}$$

where q_s^* is the concentration of substrate in the solid phase which would be in equilibrium with that in the liquid phase, i.e.,

$$q_s^* = K_{ds}C_s \tag{4.8}$$

Substituting this expression into equation (4.7) yields

$$(-j_s^s) = k_s\left(\frac{q_s}{K_{ds}} - C_s\right) \tag{4.9}$$

where

$$k_s = k_s'K_{ds} \tag{4.10}$$

Substitution of equation (4.9) into equations (4.6) and (4.4) results, respectively, in

$$\epsilon\frac{\partial C_s}{\partial t} = \epsilon E\ \frac{\partial^2 C_s}{\partial x^2} - \epsilon v\ \frac{\partial C_s}{\partial x} + \epsilon r_s^L + \rho r_s^{sf} + ak_s\left(\frac{q_s}{K_{ds}} - C_s\right) \tag{4.11}$$

$$\rho\frac{\partial q_s}{\partial t} = -\ ak_s\left(\frac{q_s}{K_{ds}} - C_s\right) \tag{4.12}$$

The flux of oxygen, j_o^s, is negligible because the solid phase hardly adsorbs oxygen; thus,

$$\frac{\partial q_o}{\partial t} = 0 \tag{4.13}$$

$$\epsilon \frac{\partial C_o}{\partial t} = \epsilon E \frac{\partial^2 C_o}{\partial x^2} - \epsilon v \frac{\partial C_o}{\partial x} + \epsilon r_o^L + \rho r_o^{sf} \qquad (4.14)$$

The rates of exchange between biomass in the form of immobile microcolonies and that in the form of suspended microorganisms are not controlled by transport within the pore network of the solid phase because the microcolonies are mainly at the interface between the liquid and solid phases. Thus, a local adsorption-desorption equilibrium exists, which can be expressed as

$$q_b = K_{db} C_b \qquad (4.15)$$

where K_{db} is the partition coefficient of biomass. Substituting equation (4.15) into equation (4.4) and combining the resultant expression with equation (4.6) lead to a single expression, i.e., (see Appendix I)

$$\epsilon R_b \frac{\partial C_b}{\partial t} = \epsilon E \frac{\partial^2 C_b}{\partial x^2} - \epsilon v \frac{\partial C_b}{\partial x} + \epsilon r_b^L + \rho r_b^{sf} \qquad (4.16)$$

where

$$R_b = 1 + \frac{\rho K_{db}}{\epsilon} \qquad (4.17)$$

This expression is termed as the retardation factor of biomass.

The reaction terms in equations (4.11), (4.14) and (4.16) can be expressed in terms of the Monod model (see, e.g., Bailey and Ollis, 1987). The rate of biomass growth in the form of the suspended microorganisms in the liquid phase, r_b^L, is expressed as

$$r_b^L = \mu_m C_b \left(\frac{C_s}{K_s+C_s}\right)\left(\frac{C_o}{K_o+C_o}\right) - k_d C_b \qquad (4.18)$$

where the first term on the right-hand side is for the growth and the second term is for the decay. The rate of biomass growth in the form of microcolonies at the interface, r_b^{sf}, is expressed as

$$r_b^{sf} = \mu_m q_b \left(\frac{C_s}{K_s+C_s}\right)\left(\frac{C_o}{K_o+C_o}\right) - k_d q_b \qquad (4.19)$$

where q_b is the concentration of microcolonies at the interface, based on the mass of the solid phase. Note that as stated in assumption g, the concentrations of substrate and oxygen extracted by the microcolonies are equal to those in the bulk of the liquid phase. Similarly, the rate of substrate degradation by the suspended microorganisms in the liquid phase, $-r_s^L$, is

$$(-r_s^L) = \frac{\mu_m}{Y_s} C_b \left(\frac{C_s}{K_s+C_s}\right)\left(\frac{C_o}{K_o+C_o}\right) \qquad (4.20)$$

The rate of substrate degradation by the microcolonies at the interface, $-r_s^{sf}$, is

$$(-r_s^{sf}) = \frac{\mu_m}{Y_s} q_b \left(\frac{C_s}{K_s+C_s}\right)\left(\frac{C_o}{K_o+C_o}\right) \qquad (4.21)$$

The rate of oxygen consumption in the bulk of the liquid phase, $-r_o^L$, and that at the interface, $-r_o^{sf}$, are expressed, respectively, as

$$(-r_o^L) = \frac{\mu_m}{Y_o} C_b \left(\frac{C_s}{K_s+C_s}\right)\left(\frac{C_o}{K_o+C_o}\right) \qquad (4.22)$$

$$(-r_o^{sf}) = \frac{\mu_m}{Y_o} q_b \left(\frac{C_s}{K_s+C_s}\right)\left(\frac{C_o}{K_o+C_o}\right) \qquad (4.23)$$

Substituting the above kinetic expressions and the equilibrium relation of biomass, equation (4.15), into equations (4.11), (4.14) and (4.16) gives rise, respectively, to (see Appendix II)

$$\frac{\partial C_s}{\partial t} = E \frac{\partial^2 C_s}{\partial x^2} - v\frac{\partial C_s}{\partial x} + \frac{k_s a}{\epsilon}\left(\frac{q_s}{K_{ds}} - C_s\right) - \frac{\mu_m}{Y_s} R_b C_b \left(\frac{C_s}{K_s + C_s}\right)\left(\frac{C_o}{K_o + C_o}\right) \tag{4.24}$$

$$\frac{\partial C_o}{\partial t} = E \frac{\partial^2 C_o}{\partial x^2} - v\frac{\partial C_o}{\partial x} - \frac{\mu_m}{Y_o} R_b C_b \left(\frac{C_s}{K_s + C_s}\right)\left(\frac{C_o}{K_o + C_o}\right) \tag{4.25}$$

$$R_b \frac{\partial C_b}{\partial t} = E \frac{\partial^2 C_b}{\partial x^2} - v\frac{\partial C_b}{\partial x} + \mu_m R_b C_b \left(\frac{C_s}{K_s + C_s}\right)\left(\frac{C_o}{K_o + C_o}\right) - k_d R_b C_b \tag{4.26}$$

These three equations together with equation (4.12) rewritten as

$$\frac{\partial q_s}{\partial t} = -\frac{k_s a}{\rho}\left(\frac{q_s}{K_{ds}} - C_s\right) \tag{4.27}$$

constitute the nonequilibrium model.

4.1.4 Dimensional Analysis

To better understand the effects of the model parameters on the solution, it is desirable to rewrite equations (4.24) through (4.27) in dimensionless form. For this purpose, the following dimensionless variables are defined.

$$\theta = \frac{tv}{L} \tag{4.28}$$

$$X = \frac{x}{L} \tag{4.29}$$

$$\bar{C}_s = \frac{C_s}{C^*_{s0}} \tag{4.30}$$

$$\bar{C}_o = \frac{C_o}{C_{of}} \tag{4.31}$$

$$\bar{C}_b = \frac{C_b R_b}{C^*_{s0} R_s Y_s} \tag{4.32}$$

$$\bar{q}_s = \frac{q_s}{q_{s0}} = \frac{q_s / K_{ds}}{C^*_{s0}} \tag{4.33}$$

In these definitions, C_{of} is the concentration of oxygen in the feed solution and C^*_{s0} is the concentration of substrate in the liquid phase which would be in equilibrium with the initial concentration of substrate in the solid phase, q_{s0}. Note that in the definition of the dimensionless concentration of biomass, $\bar{C}_b$, the numerator stands for the total biomass in the forms of both suspended microorganisms in the liquid phase and microcolonies at the interface, and the denominator stands for the maximum quantity of biomass produceable from the available substrate deposited in the bed. Substitution of the dimensionless variables into equations (4.24) through (4.27) results, respectively, in

$$\frac{\partial \bar{C}_s}{\partial \theta} = \frac{1}{Pe} \frac{\partial^2 \bar{C}_s}{\partial X^2} - \frac{\partial \bar{C}_s}{\partial X} + St_m(\bar{q}_s - \bar{C}_s) - N_{r,1} R_s \bar{C}_b \left(\frac{\bar{C}_s}{\bar{K}_s + \bar{C}_s}\right)\left(\frac{\bar{C}_o}{\bar{K}_o + \bar{C}_o}\right) \tag{4.34}$$

$$\frac{\partial \bar{C}_o}{\partial \theta} = \frac{1}{Pe} \frac{\partial^2 \bar{C}_o}{\partial X^2} - \frac{\partial \bar{C}_o}{\partial X} - N_{r,1} W \bar{C}_b \left(\frac{\bar{C}_s}{\bar{K}_s + \bar{C}_s}\right)\left(\frac{\bar{C}_o}{\bar{K}_o + \bar{C}_o}\right) \tag{4.35}$$

$$\frac{\partial \bar{C}_b}{\partial \theta} = \frac{1}{R_b Pe}\frac{\partial^2 \bar{C}_b}{\partial X^2} - \frac{1}{R_b}\frac{\partial \bar{C}_b}{\partial X} + N_{r,1}\bar{C}_b\left(\frac{\bar{C}_s}{\bar{K}_s+\bar{C}_s}\right)\left(\frac{\bar{C}_o}{\bar{K}_o+\bar{C}_o}\right) - N_{r,2}\bar{C}_b \quad (4.36)$$

$$\frac{\partial \bar{q}_s}{\partial \theta} = -\frac{St_m}{R_s - 1}(\bar{q}_s - \bar{C}_s) \quad (4.37)$$

where

$$Pe = \frac{Lv}{E} \quad (4.38)$$

$$N_{r,1} = \frac{\mu_m L}{v} \quad (4.39)$$

$$N_{r,2} = \frac{k_d L}{v} \quad (4.40)$$

$$St_m = \frac{k_s a L}{v\epsilon} \quad (4.41)$$

$$R_s = 1 + \frac{\rho K_{ds}}{\epsilon} \quad (4.42)$$

$$\bar{K}_s = \frac{K_s}{C^*_{s0}} \quad (4.43)$$

$$\bar{K}_o = \frac{K_o}{C_{of}} \quad (4.44)$$

$$W = \frac{C^*_{s0} R_s Y_s}{C_{of} Y_o} \quad (4.45)$$

Among the dimensionless numbers, $N_{r,1}$ and $N_{r,2}$, defined in equations (4.39) and (4.40), respectively, are known as the reaction units; the former is for the growth of biomass and the latter is for the decay of biomass. These numbers reflect the magnitudes of reaction rates. R_s, defined in equation (4.42), is the retardation factor of substrate. W, defined in equation (4.45), is the ratio of the maximum quantity of biomass produceable from the available substrate

to that of biomass produceable from the available oxygen; thus, it can be termed as the oxygen supply number.

For a soil bed with a depth of L and a cross-sectional area of A the quantity of substrate initially deposited in the liquid phase is $LA\epsilon C^*_{s0}$ and the quantity of substrate initially deposited in the solid phase is $LA\rho q_{s0}$. The sum of these two quantities is the total quantity of the substrate in the bed, $LA\epsilon C^*_{s0}R_s$, where R_s is defined in equation (4.42). Thus, the maximum quantity of biomass produceable from the substrate is $LA\epsilon C^*_{s0}R_sY_s$. In case neither substrate nor oxygen flows out of the bed, the maximum quantity of biomass produceable from the substrate is equal to that from the oxygen which is equal to $t_m vA\epsilon C_{of}Y_o$, where v is the pore velocity of water and t_m is the minimum time required for completing the biodegradation process under the conditions of plug flow and negligible mass transfer resistance. This and equation (4.45) lead to

$$\frac{t_m v}{L} = \frac{C^*_{s0}R_sY_s}{C_{of}Y_o} = W \qquad (4.46)$$

Thus, W can also be defined as the minimum dimensionless time for completing a biodegradation process.

The Damköhler number for bioremediation of contaminated soil can be defined by dividing equation (4.39) with equation (4.41), i.e.,

$$Da = \frac{N_{r,1}}{St_m} = \frac{\mu_m}{k_s(a/\epsilon)} \qquad (4.47)$$

This number signifies the ratio of the maximum specific growth rate to the maximum substrate transfer rate.

When the aqueous solubility of the substrate in bioremediation of contaminated soil is sufficiently low so that C^*_{s0} is much less than the saturation constant of substrate, K_s, the dimensionless saturation constant of substrate, $\bar{K}_s$, will be much greater than unity. Consequently, a modified Damköhler number, Da', is defined as follows:

$$Da' = \frac{\mu_m/\bar{K}_s}{k_s(a/\epsilon)} \tag{4.48}$$

Note that Da' is inversely proportional to the mass transfer coefficient of substrate, k_s.

4.2 SOLUTION ALGORITHM AND NUMERICAL SOLUTION

The model equations developed in the preceding section consist of three convection-dispersion partial differential equations (PDE's) and one ordinary differential equation (ODE). As discussed in Chapter 2, two major difficulties are encountered in solving these equations. One is that numerical solution of a convection-dispersion PDE is adversely affected by numerical oscillations and diffusion if the convection term is more dominant than the dispersion term. The other is that the three PDE's are coupled through

the nonlinear reaction terms, and they are also coupled with the ODE. These difficulties have been overcome by resorting to the three-point backward finite difference method (TPB method), developed in Chapter 2. The numerical procedure for solving equations (4.34) through (4.37) is given below.

Equations (4.34) through (4.36) can be compactly rewritten as

$$\frac{\partial \bar{C}_i}{\partial \theta} = P_{1,i} \frac{\partial^2 \bar{C}_i}{\partial X^2} - P_{2,i} \frac{\partial \bar{C}_i}{\partial X} + f_i, \quad i = s, o, b \qquad (4.49)$$

where subscript i refers to component i, and $P_{1,i}$ and $P_{2,i}$ are the coefficients for the dispersion and convection terms, respectively. The nonlinear reaction terms in equation (4.49), f_i, i=s, o, b, can be expressed as

$$f_s(\bar{C}_s,\bar{C}_o,\bar{C}_b,\bar{q}_s) = St_m(\bar{q}_s - \bar{C}_s) - N_{r,1} R_s \bar{C}_b \left(\frac{\bar{C}_s}{\bar{K}_s+\bar{C}_s}\right)\left(\frac{\bar{C}_o}{\bar{K}_o+\bar{C}_o}\right) \qquad (4.50)$$

$$f_o(\bar{C}_s,\bar{C}_o,\bar{C}_b) = - N_{r,1} W \bar{C}_b \left(\frac{\bar{C}_s}{\bar{K}_s+\bar{C}_s}\right)\left(\frac{\bar{C}_o}{\bar{K}_o+\bar{C}_o}\right) \qquad (4.51)$$

$$f_b(\bar{C}_s,\bar{C}_o,\bar{C}_b) = N_{r,1} \bar{C}_b \left(\frac{\bar{C}_s}{\bar{K}_s+\bar{C}_s}\right)\left(\frac{\bar{C}_o}{\bar{K}_o+\bar{C}_o}\right) - N_{r,2} \bar{C}_b \qquad (4.52)$$

According to Chapter 2, the finite difference approximation of equation (4.49) can be written as

$$\begin{aligned} &(-r_{1,i} - 2r_{2,i})(\bar{C}_i)^{n+1}_{j-1} + (3 + 2r_{1,i} + 2r_{2,i})(\bar{C}_i)^{n+1}_{j} \\ &\quad - r_{1,i}(\bar{C}_i)^{n+1}_{j+1} \\ &= -r_{2,i}(\bar{C}_i)^{n}_{j-2} + 2r_{2,i}(\bar{C}_i)^{n}_{j-1} + (4 - r_{2,i})(\bar{C}_i)^{n}_{j} \end{aligned}$$

$$-(\bar{C}_i)_j^{n-1} + 2\Delta\theta\, f_i^{n+1}, \qquad (4.53)$$

$$i = s, o, b$$

where

$$r_{1,i} = \frac{2P_{1,i}\Delta\theta}{\Delta X^2} \qquad (4.54)$$

$$r_{2,i} = \frac{P_{2,i}\Delta\theta}{\Delta X} \qquad (4.55)$$

Equation (4.53) is a system of nonlinear equations due to the existence of the nonlinear reaction term, f_i^{n+1}. According to the two-step expansion given in equation (2.43), f_i^{n+1} can be expressed as

$$f_i^{n+1} = f_i^{n-1} + 2\left(\frac{\partial f_i^n}{\partial\theta}\right)\Delta\theta \qquad (4.56)$$

The derivatives of f_i's with respect to θ in equation (4.56) are obtained as follows:

$$\frac{\partial f_s}{\partial\theta} = \frac{\partial f_s}{\partial\bar{C}_s}\frac{\partial\bar{C}_s}{\partial\theta} + \frac{\partial f_s}{\partial\bar{C}_o}\frac{\partial\bar{C}_o}{\partial\theta} + \frac{\partial f_s}{\partial\bar{C}_b}\frac{\partial\bar{C}_b}{\partial\theta} + \frac{\partial f_s}{\partial\bar{q}_s}\frac{\partial\bar{q}_s}{\partial\theta} \qquad (4.57)$$

$$\frac{\partial f_o}{\partial\theta} = \frac{\partial f_o}{\partial\bar{C}_s}\frac{\partial\bar{C}_s}{\partial\theta} + \frac{\partial f_o}{\partial\bar{C}_o}\frac{\partial\bar{C}_o}{\partial\theta} + \frac{\partial f_o}{\partial\bar{C}_b}\frac{\partial\bar{C}_b}{\partial\theta} \qquad (4.58)$$

$$\frac{\partial f_b}{\partial\theta} = \frac{\partial f_b}{\partial\bar{C}_s}\frac{\partial\bar{C}_s}{\partial\theta} + \frac{\partial f_b}{\partial\bar{C}_o}\frac{\partial\bar{C}_o}{\partial\theta} + \frac{\partial f_b}{\partial\bar{C}_b}\frac{\partial\bar{C}_b}{\partial\theta} \qquad (4.59)$$

The derivatives of f_i's with respect to $\bar{C}_i$ in equations (4.57) through (4.59) are obtained analytically from equations (4.50) through (4.52); $\partial\bar{C}_i/\partial\theta$ can be calculated from the finite difference approximation of equations (4.34) through (4.36). Meanwhile, the evaluation of $\partial\bar{q}_s/\partial\theta$ in

equation (4.57) can be directly obtained from equation (4.37). With all these derivatives available, f_i^{n+1} can be evaluated from equation (4.56); subsequently, $\bar{C}_i^{n+1}$ is obtained with the tridiagonal method from equation (4.53).

After equations (4.34) through (4.36) are solved with the TPB method at each time step, the ODE among the model equations, equation (4.37), can be solved for $\bar{q}_i^{n+1}$ with the second order Runge-Kutta method. The resultant scheme is

$$\bar{q}_s^{n+1} = b_1 \bar{C}_s^{n+1} + b_2 C_s^n + b_3 \bar{q}_s^n \tag{4.60}$$

where

$$b_1 = \frac{\Delta\theta St_m}{2\bar{K}_{ds}} \tag{4.61}$$

$$b_2 = \frac{\Delta\theta St_m}{2\bar{K}_{ds}} \left(1 - \frac{\Delta\theta St_m}{\bar{K}_{ds}} \right) \tag{4.62}$$

$$b_3 = 1 - \frac{\Delta\theta St_m}{\bar{K}_{ds}} + \frac{(\Delta\theta St_m)^2}{2\bar{K}_{ds}^2} \tag{4.63}$$

The starting algorithm is also given in Chapter 2.

Two classes of numerical simulation have been conducted with the developed algorithm. One is for the once-through operation for which the initial and boundary conditions are

At $\theta = 0$, $\bar{C}_s(0,X) = 1.00$, $\bar{q}_s(0,X) = 1.00$

$\bar{C}_o(0,X) = 0.05$, $\bar{C}_b(0,X) = 0.01$

At $X = 0$, $\bar{C}_i(\theta,0) = (\bar{C}_i)_{o+} - \frac{1}{Pe} \left(\frac{\partial \bar{C}_i}{\partial X}\right)_{o+}$, $i = s, o, b$

where

$$\bar{C}_s(\theta,0) = 0.00$$

$$\bar{C}_o(\theta,0) = 1.00$$

$$\bar{C}_b(\theta,0) = 0.01$$

$$\text{At } X = 1, \quad \frac{\partial \bar{C}_i}{\partial X} = 0, \qquad i = s, o, b$$

The other is for the recycle operation, in which the effluent containing unreacted substrate is recycled to the top of the bed to eliminate the substrate, i.e., contaminants, to the maximum extent possible. For this operation, the initial conditions and the boundary conditions at X=1 are the same as those for the once-through operation. The boundary conditions at the inlet of the bed are

$$\text{At } X = 0, \quad \bar{C}_i(\theta,0) = (\bar{C}_i)_{o+} - \frac{1}{Pe}\left(\frac{\partial \bar{C}_i}{\partial X}\right)_{o+}, \quad i = s, o, b$$

where

$$\bar{C}_s(\theta,0) = \bar{C}_s(\theta-\Delta\theta, 1)$$

$$\bar{C}_o(\theta,0) = 1.00$$

$$\bar{C}_b(\theta,0) = \bar{C}_b(\theta-\Delta\theta, 1)$$

where the residence time of the recycle stream is assumed to be very short and equal to $\Delta\theta$, the dimensionless temporal step size for the numerical integration. It is also assumed that no reaction takes place in the recycle stream. The parameters used in the simulation are given in Table 4.1.

4.3 RESULTS AND DISCUSSION

The results have been obtained from simulating both once-through and recycle operations. Analysis of the dynamics of the once-through operation enables us to determine the effects of various model parameters on the rate of biodegradation. Insight into the in situ bioremediation process can be gained through understanding the dynamics of the recycle operation.

4.3.1 Dynamics of the Once-Through Operation

The effects of model parameters on the rate of biodegradation have been analyzed by focussing on the modified Damköhler number, Da', the retardation factor of substrate, R_s, and the oxygen supply number, W.

Figures 4.2 through 4.4 reveal the effect of Da' on the rate of biodegradation. Da' reflects the ratio of the maximum specific growth rate to specific substrate transfer rate. When the maximum specific growth rate is fixed, the larger the Da', the smaller the transfer rate, or the larger the resistance to substrate transport. When Da' is equal to 1, $\bar{C}_s$ is much lower than $\bar{q}_s$ (see Figure 4.2). The difference between $\bar{C}_s$ and $\bar{q}_s$ represents the departure of the state of the system from its equilibrium state, which is determined by the rate of substrate transport. When Da' decreases to

0.5, the rate of substrate transport increases, but the difference between $\bar{C}_s$ and $\bar{q}_s$ continues to be appreciable (see Figure 4.3). When Da' further decreases to 0.1, the rate of substrate transport becomes so fast that $\bar{C}_s$ approaches to $\bar{q}_s$. A comparison between Figures 4.2 and 4.4 shows the smaller the Da', the faster the rate of biodegradation.

The rate of biodegradation is also affected by the retardation factor of substrate, R_s. By definition, R_s signifies the magnitude of the equilibrium constant of substrate, K_{ds}. The larger the R_s, the larger the K_{ds}, and, from equation (4.7) or (4.9), the smaller the concentration gradient, or the driving force. A comparison between Figures 4.4 and 4.5 indicates that when R_s increases from 20 to 60 and Da' remains at 0.1, the difference between $\bar{C}_s$ and $\bar{q}_s$ increases, or the nonequilibrium behavior is enhanced. This is because the rate of substrate transport is decreased. R_s in bioremediation of contaminated soil may be larger than 60. The larger the R_s, the slower the rate of substrate transport, and thus, the slower the rate of biodegradation.

The oxygen supply number, W, is another factor affecting the rate of biodegradation; it signifies the ratio of the maximum quantity of biomass produceable from the available substrate to that from the available oxygen. The larger the W, the lesser the available oxygen. Figures 4.3 through 4.5 show that when W is 12.5 and Da' or R_s is small,

the oxygen in the liquid phase is rapidly consumed and the insufficient oxygen supply through the liquid phase becomes rate-limiting. A comparison between Figures 4.3 and 4.6 reveals that when W decreases to 6 from 12.5, the effect of the insufficient oxygen supply becomes less profound and the resistance to the substrate desorption becomes increasingly dominant. Note that the increase in R_s can change the rate-limiting step for the same W. For instance, as R_s increases from 20 to 80 and W remains 12.5, we see from Figures 4.3 and 4.7 that the difference between $\bar{C}_s$ and $\bar{q}_s$ increases significantly and the value of $\bar{C}_s$ becomes very low, indicating that the resistance to the substrate desorption is rate-limiting.

4.3.2 Dynamics of the Recycle Operation

The once-through operation discussed in the preceding subsection has demonstrated the effects of substrate transport resistance and insufficient oxygen supply on the rate of biodegradation. However, the once-through operation is seldom employed because the contaminants would flow into the groundwater underneath the bed. The recycle operation provides a means to eliminate the substrate, i.e., contaminants, to the maximum extent possible.

The simulated concentration profiles are plotted at different dimensionless time in Figures 4.8 through 4.11.

At θ of 2 and 4, three distinct reaction zones are observed in the bed (Figures 4.8 and 4.9). In the upper zone, the concentrations of both oxygen and recycled substrate are high, thereby exhibiting a high rate of biodegradation and steep decline in the concentration profiles. In the middle zone, the rate of biodegradation becomes moderate because it is constrained by the low concentrations of both oxygen and substrate in the liquid phase; consequently, the concentration profiles become rather flat. Oxygen is totally consumed in the lower zone, and thus, degradation of substrate ceases. Figure 4.10 demonstrates that at θ of 6, the middle zone expands substantially as the result of biodegradation; meanwhile, the lower zone shrinks significantly. The concentration profiles at θ=8 (Figure 4.11) indicate that the biodegradation process is almost complete. The fact that the oxygen supply number, W, is also equal to 8 is a proof of equation (4.46), which shows that W can also be defined as the minimum dimensionless time for completing a biodegradation process. Note that how close the dimensionless biodegradation time is to W depends on both the mass transfer resistance and hydraulic dispersion. The larger the mass transfer resistance and hydraulic dispersion, the longer the dimensionless biodegradation time. If they are negligible, the dimensionless time will be equal to W.

4.4 CONCLUDING REMARKS

A mathematical model for biodegradation of contaminants deposited in a soil bed has been developed. The transport resistance to contaminant migration within the pore network in soil particles is considered. The model equations comprise three convection-dispersion partial differential equations and one ordinary differential equation.

The numerical simulation of the once-through operation has revealed the effects of model parameters on the rate of biodegradation and has demonstrated that a nonequilibrium model is more appropriate than an equilibrium model; the rate of biodegradation may be limited not only by the insufficient oxygen supply, but also by the transport resistance to the substrate desorption. Under certain circumstances, the latter is even more dominant than the former.

The simulation of the operation involving the recycle of unreacted substrate, i.e., contaminants, has indicated that biodegradation takes place mainly in the upper part of the bed and that the oxygen supply factor, W, can serve as an estimation of the dimensionless biodegradation time if the mass transfer is relatively fast.

NOTATION

a = interfacial area per unit volume of the soil bed, L^2/L^3

C_i = concentration of component i in the liquid phase, M/L^3

C_{of} = concentration of oxygen in the feed solution, M/L^3

$\bar{C}_i$ = dimensionless concentration of component i

E = dispersion coefficient, L^2/t

j_i^L = transport flux from the liquid phase to the interface, $M/L^2/t$

j_i^s = transport flux from the interface to the bulk of the solid phase, $M/L^2/t$

k_d = reaction rate constant for the decay of biomass, t^{-1}

k_s = mass transfer coefficient of substrate, L/t

K_o = saturation constant of oxygen, M/L^3

K_s = saturation constant of substrate, M/L^3

K_{di} = dimensionless linear isotherm partition coefficient of component i

L = depth of the contaminated soil bed, L

q_i = concentration of component i in the solid phase, M/M dry soil

$\bar{q}_i$ = dimensionless concentration of component i in the solid phase

r_i^L = reaction rate in the liquid phase, $M/L^3/t$

r_i^{sf} = reaction rate at the interface, M/M dry soil/t

$R_i = 1 + \frac{\rho K_{di}}{\epsilon}$ = retardation factor for component i

v = pore velocity of the liquid, L/t

t = time, t

x = vertical position, L

X = dimensionless depth

Y_o = yield factor of oxygen

Y_s = yield factor of substrate

Greek letters

ρ = bulk density of the soil bed, M dry soil/L^3

ϵ = void fraction of the soil bed

μ_m = maximum specific growth rate of biomass, t^{-1}

θ = dimensionless time

Superscript

n = n-th time step

L = liquid phase

s = solid phase

Subscripts

i = s, o, b for substrate, oxygen and biomass, respectively

j = j-th grid point

REFERENCES

Bailey, J.E. and D.F. Ollis, Biochemical Engineering Fundamentals, pp. 373-456, McGraw-Hill, New York, 1987.

Baveye, P. and A. Valocchi, "An Evaluation of Mathematical Models of the Transport of Biologically Reacting Solutes in Saturated Soils and Aquifers," Water Resources Res., 25, 1413-1421 (1989).

Borden, R.C. and P.B. Bedient, "Transport of Dissolved Hydrocarbons Influenced by Oxygen-Limited Biodegradation, 1. Theoretical Development," Water Resources Res., 22, 1973-1982 (1986).

Iwata S., T. Tabuchi, and B. P. Warkentin, Soil-Water Interaction, Mechanisms and Applications, pp. 221-276, Marcel Dekker, New York, 1988.

Lee, M.D., J.M. Thomas, R.C. Borden, P.B. Bedient, C.H. Ward and J.T. Wilson, "Biodegradation of Aquifers Contaminated with Organic Compounds," CRC Critical Reviews in Environmental Control, 18, 29-89 (1988).

Molz, F.J., M.A. Windowson, and L.D. Benefield, "Simulation of Microbial Growth Dynamics Coupled to Nutrient and Oxygen Transport in Porous Media," Water Resources Res., 22, 1207-1216 (1986).

Valocchi, A.J., Validity of the Local Equilibrium Assumption for Modeling Sorbing Solute Transport through Homogeneous Soil, Water Resources Res., 21, 808-820 (1985).

Windowson, M.A., F.J. Molz, and L.D. Benefield, "A Numerical Transport Model for Oxygen- and Nitrate-Based Respiration Linked to Substrate and Nutrient Availability in Porous Media," Water Resources Res., 24, 1553-1565 (1988).

Table 4.1. Parameter Values for the Numerical Simulation

$N_{r,1} = 12.0$	$N_{r,2} = 0.2$
$\bar{K}_s = 3.0$	$\bar{K}_o = 0.05$
$Pe = 100$	$W = 6, 8, 12.5$
$R_s = 20, 60, 80$	$R_b = 50$
$St_m = 4, 8, 20, 40$	$D'_a = 0.1, 0.2, 0.5, 1.$

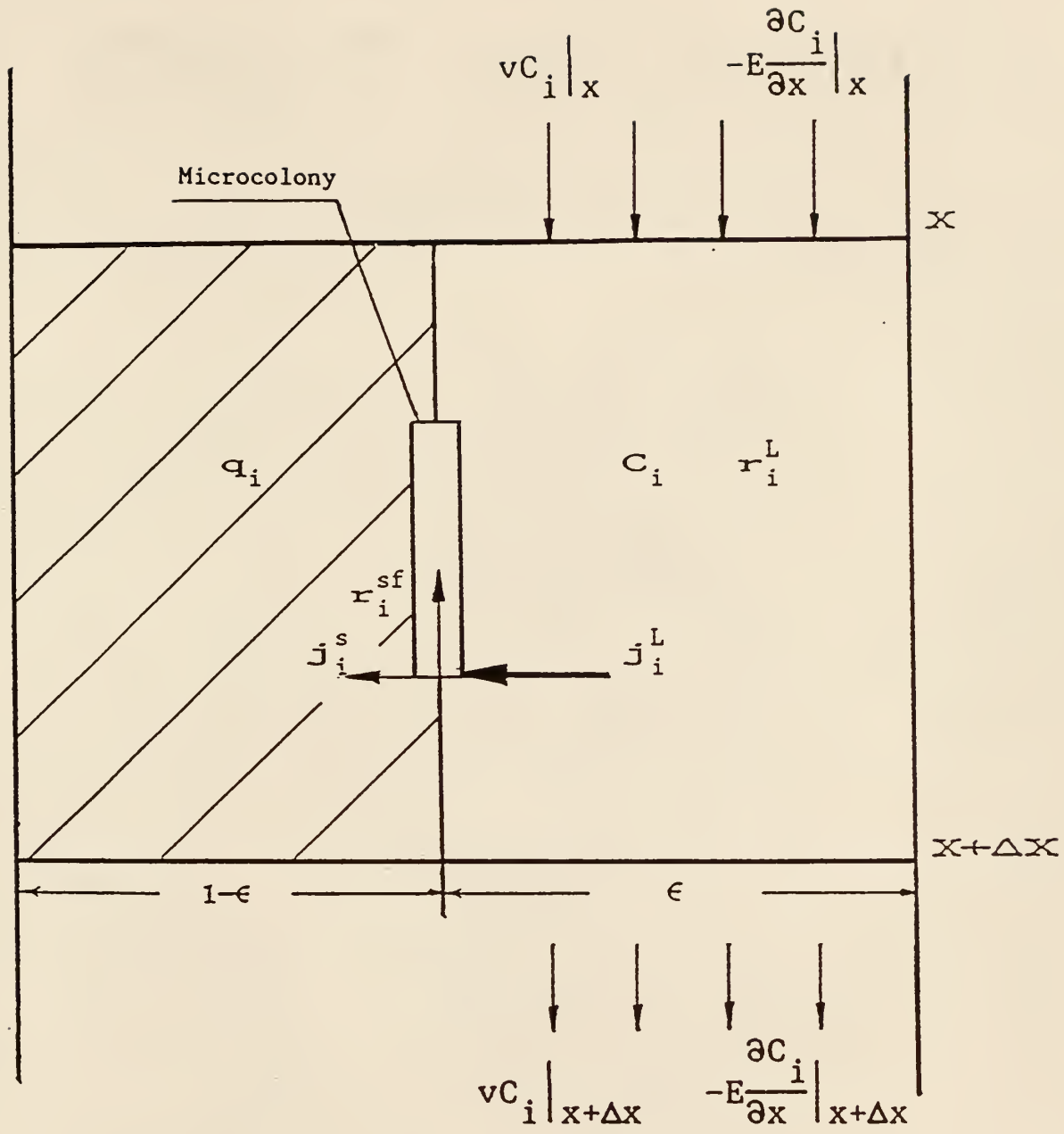

Figure 4.1. Schematic diagram of transport and biodegradation in a controlled volume.

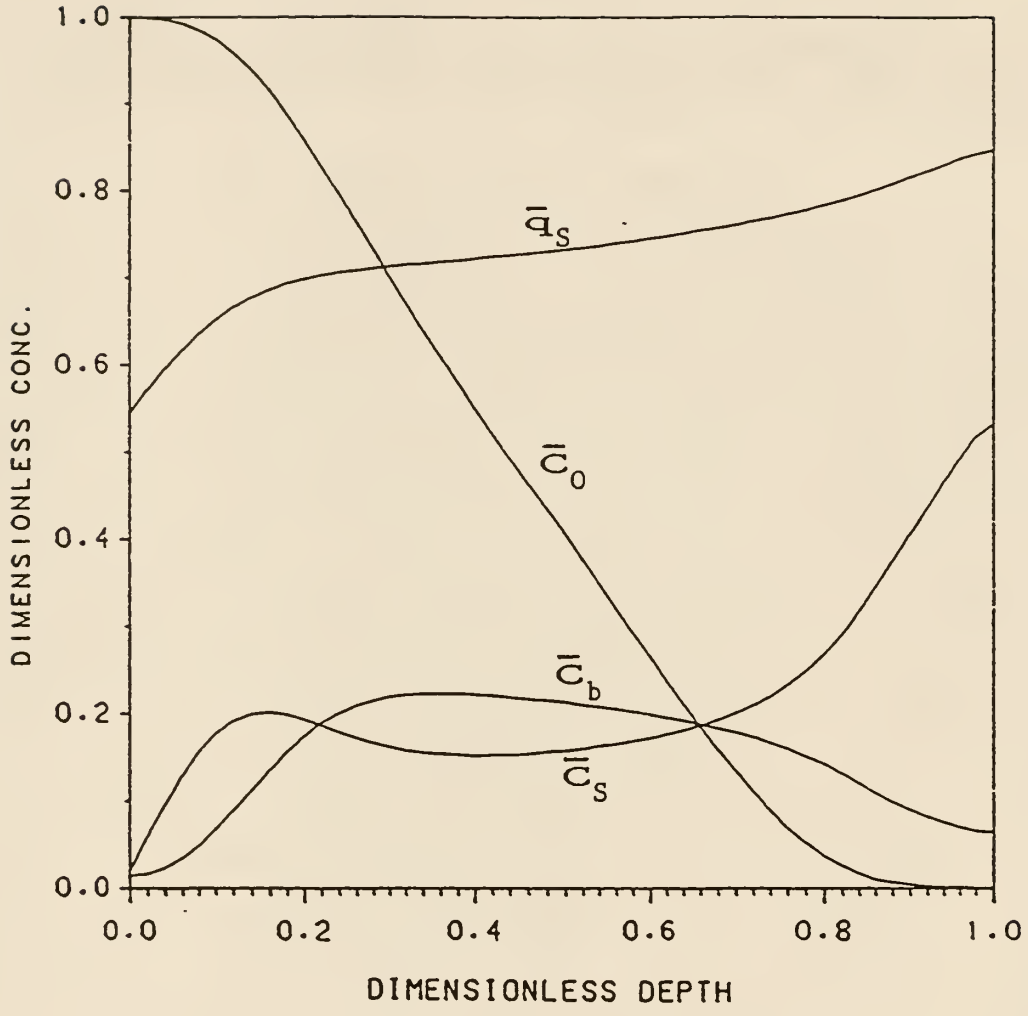

Figure 4.2. Concentration profiles for the once-through operation at θ=3: Da'=1, R_s=20 and W=12.5.

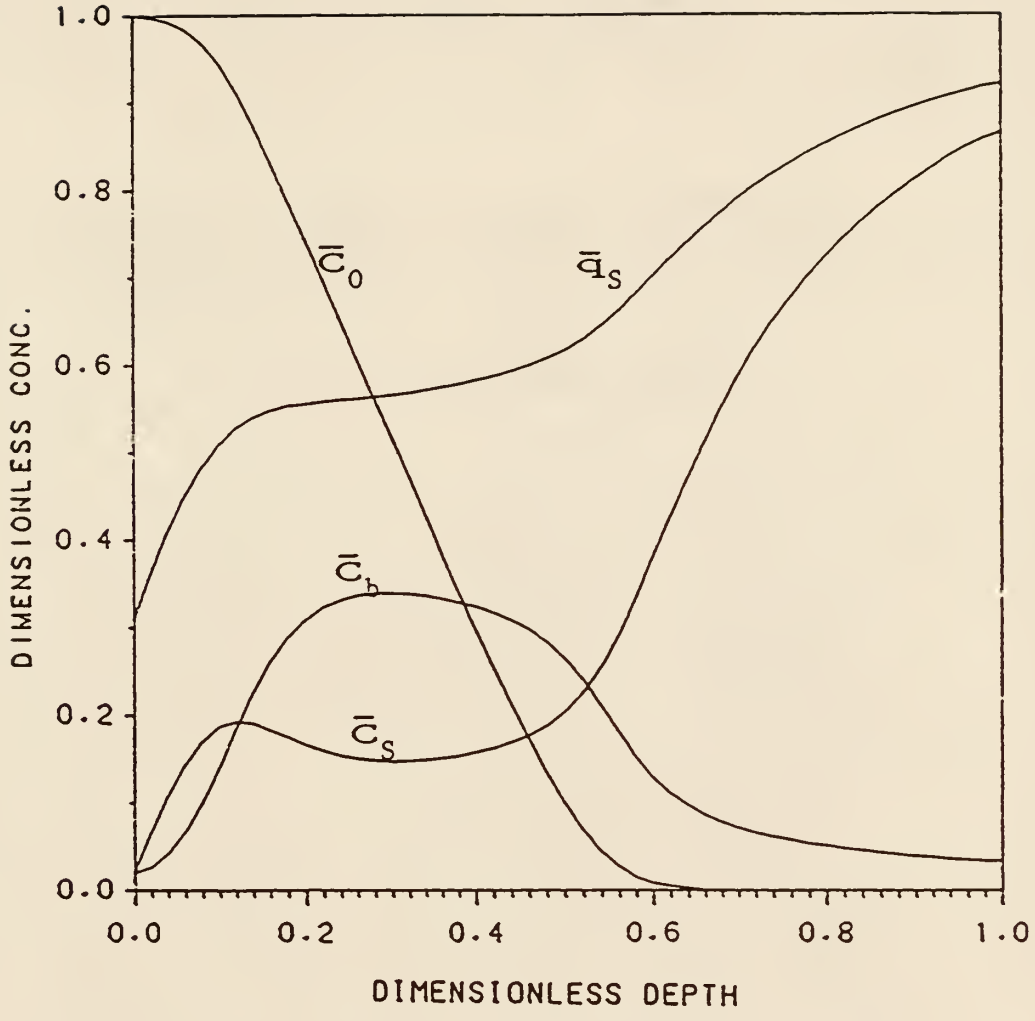

Figure 4.3. Concentration profiles for the once-through operation at θ=3: Da'=0.5, R_s=20 and W=12.5.

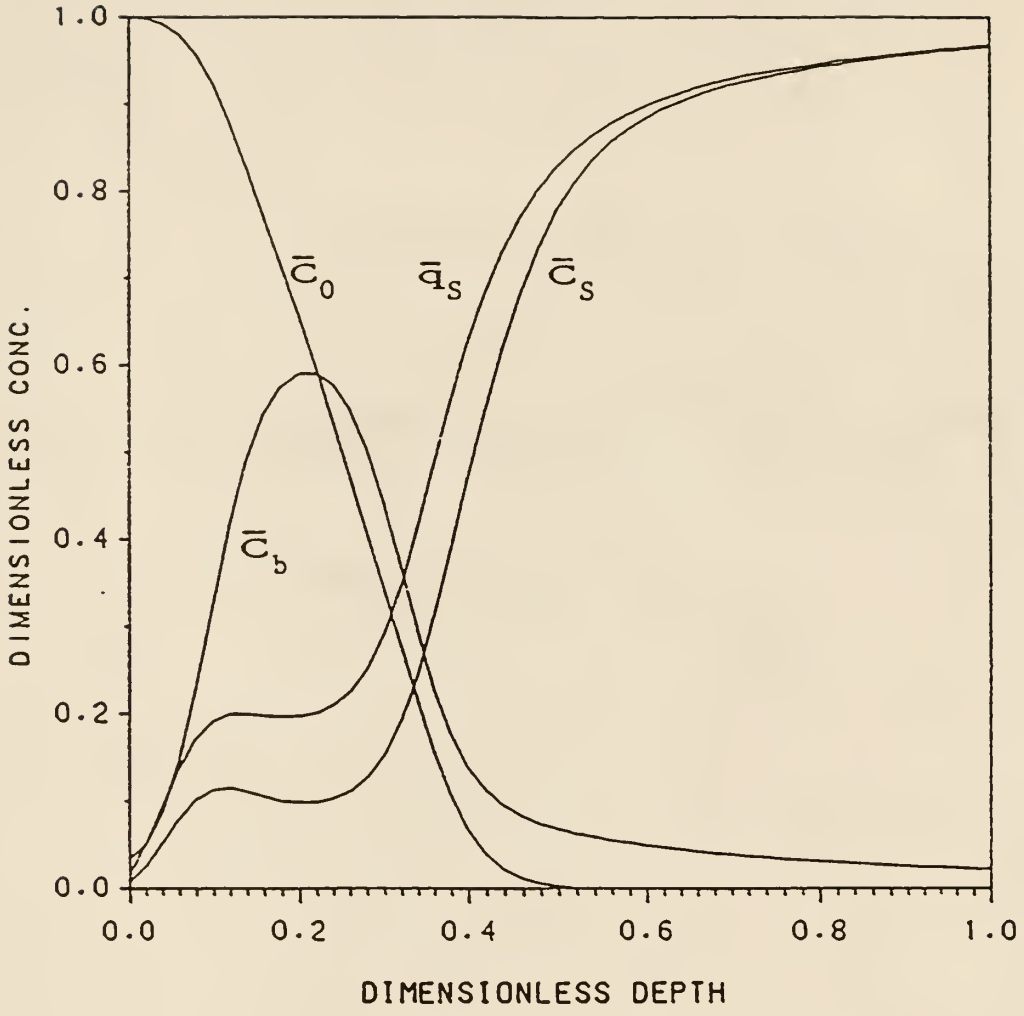

Figure 4.4. Concentration profiles for the once-through operation at Θ=3: Da'=0.1, R_s=20 and W=12.5.

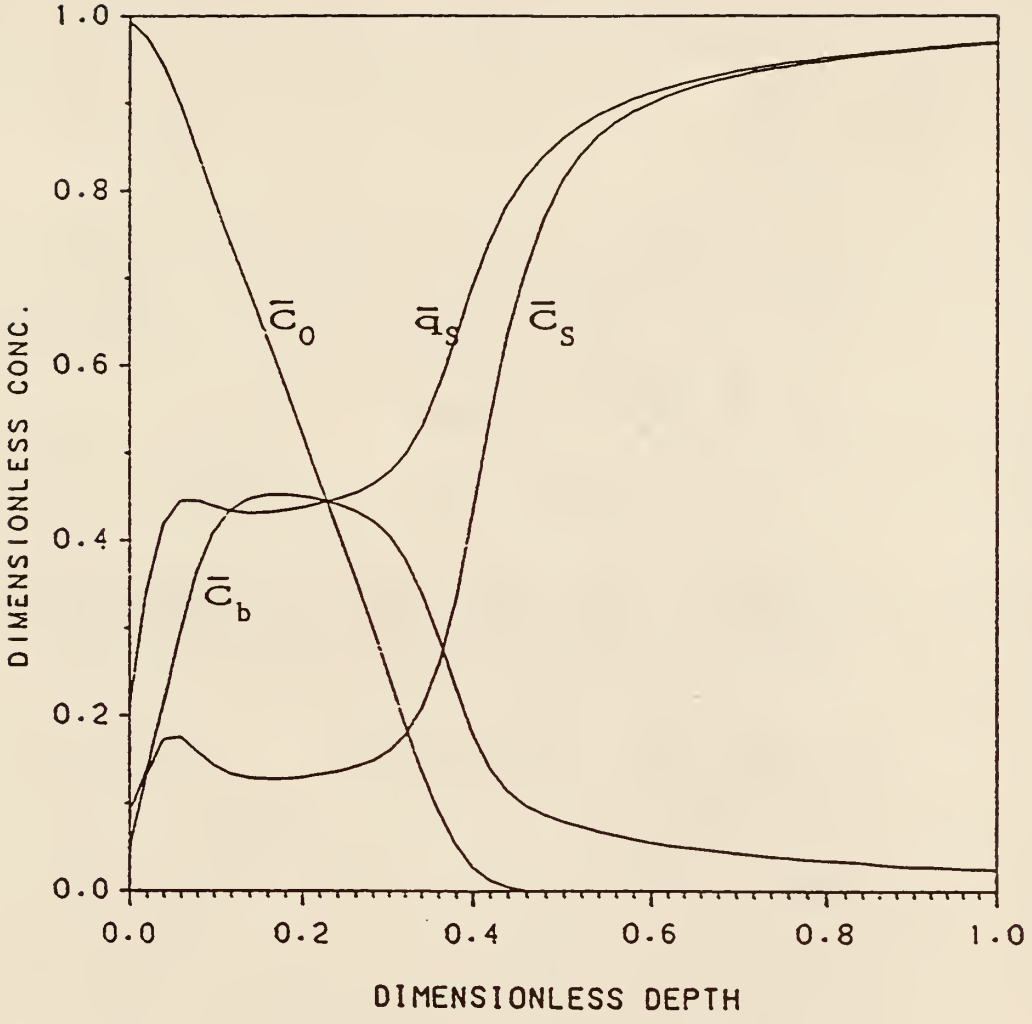

Figure 4.5. Concentration profiles for the once-through operation at θ=3: Da'=0.1, R_s=60 and W=12.5.

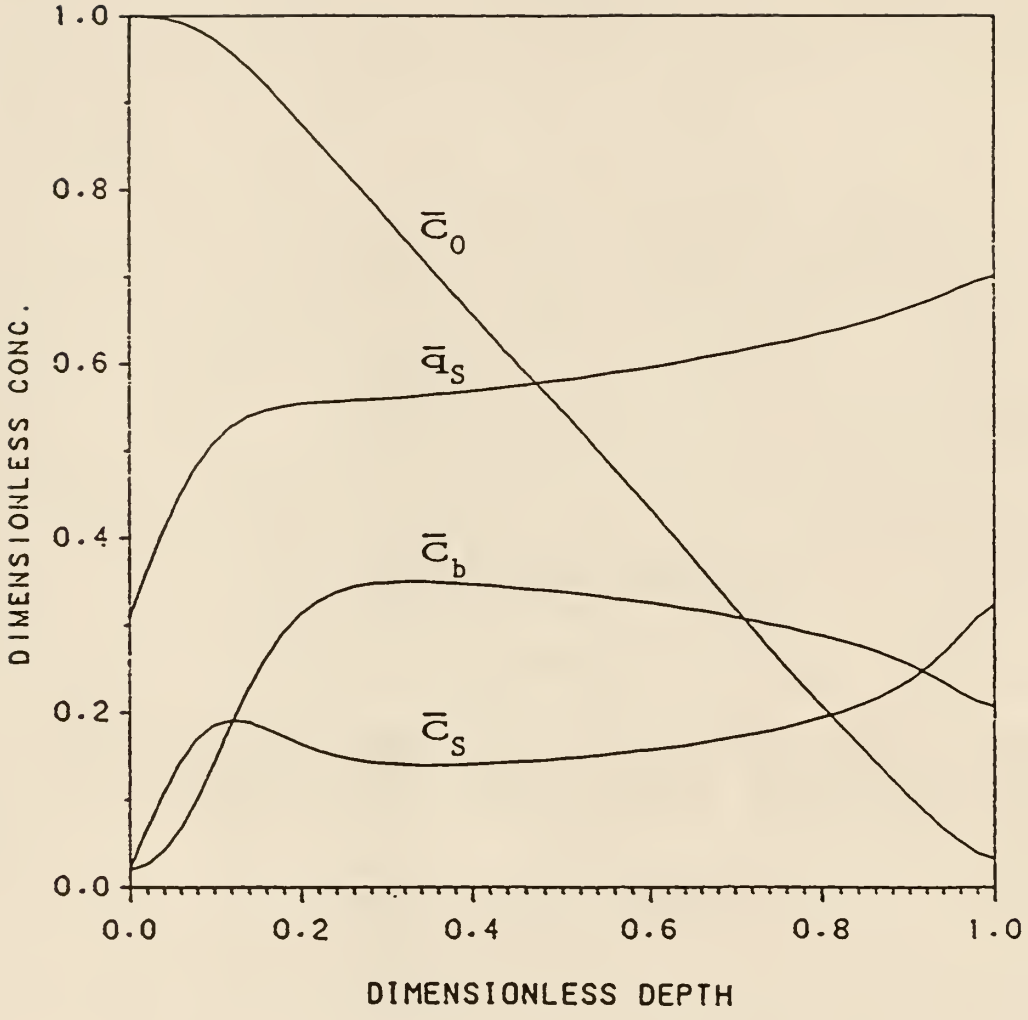

Figure 4.6. Concentration profiles for the once-through operation at Θ=3: Da'=0.5, R_s=20 and W=6.

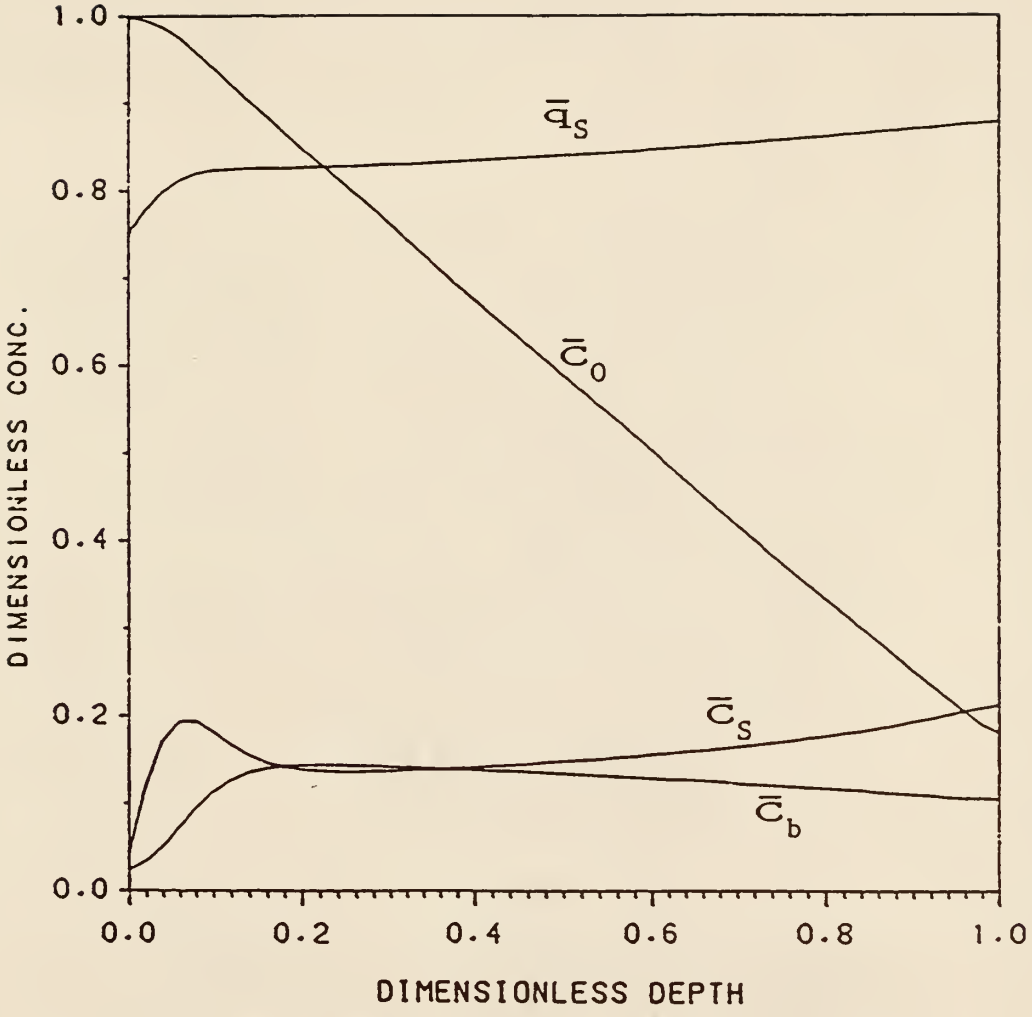

Figure 4.7. Concentration profiles for the once-through operation at Θ=3: Da'=0.5, R_s=80 and W=12.5.

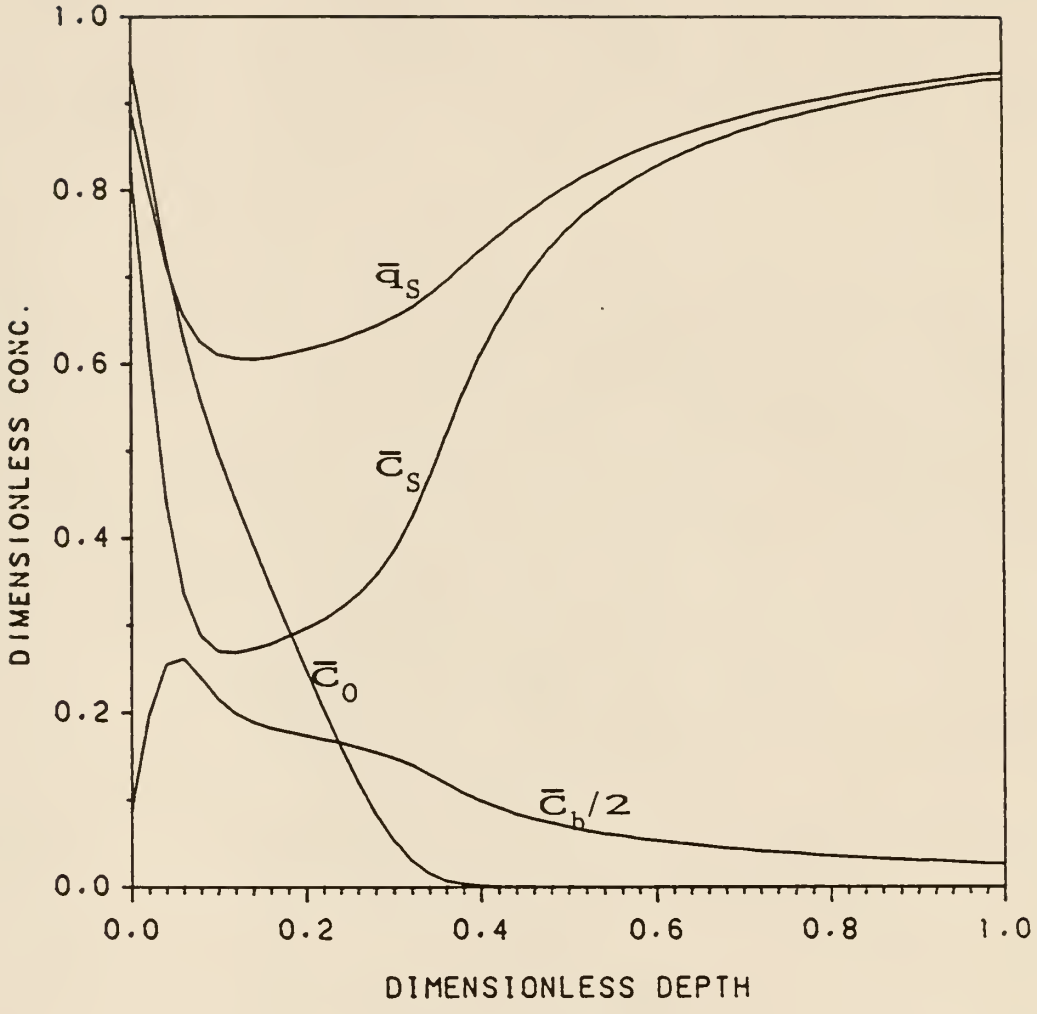

Figure 4.8. Concentration profiles for the recycle operation at θ=2: Da'=0.2, R_s=20 and W=8.

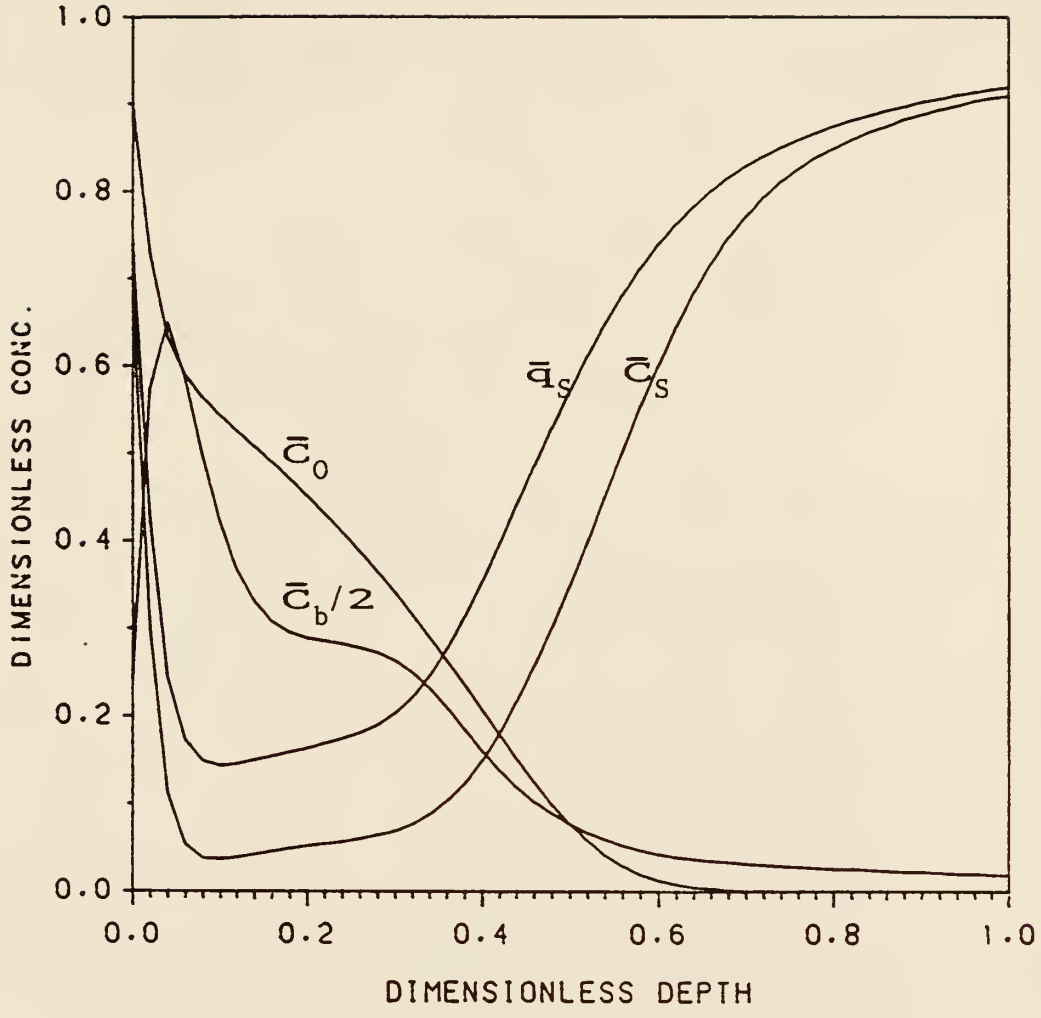

Figure 4.9. Concentration profiles for the recycle operation at $\theta=4$: $Da'=0.2$, $R_s=20$ and $W=8$.

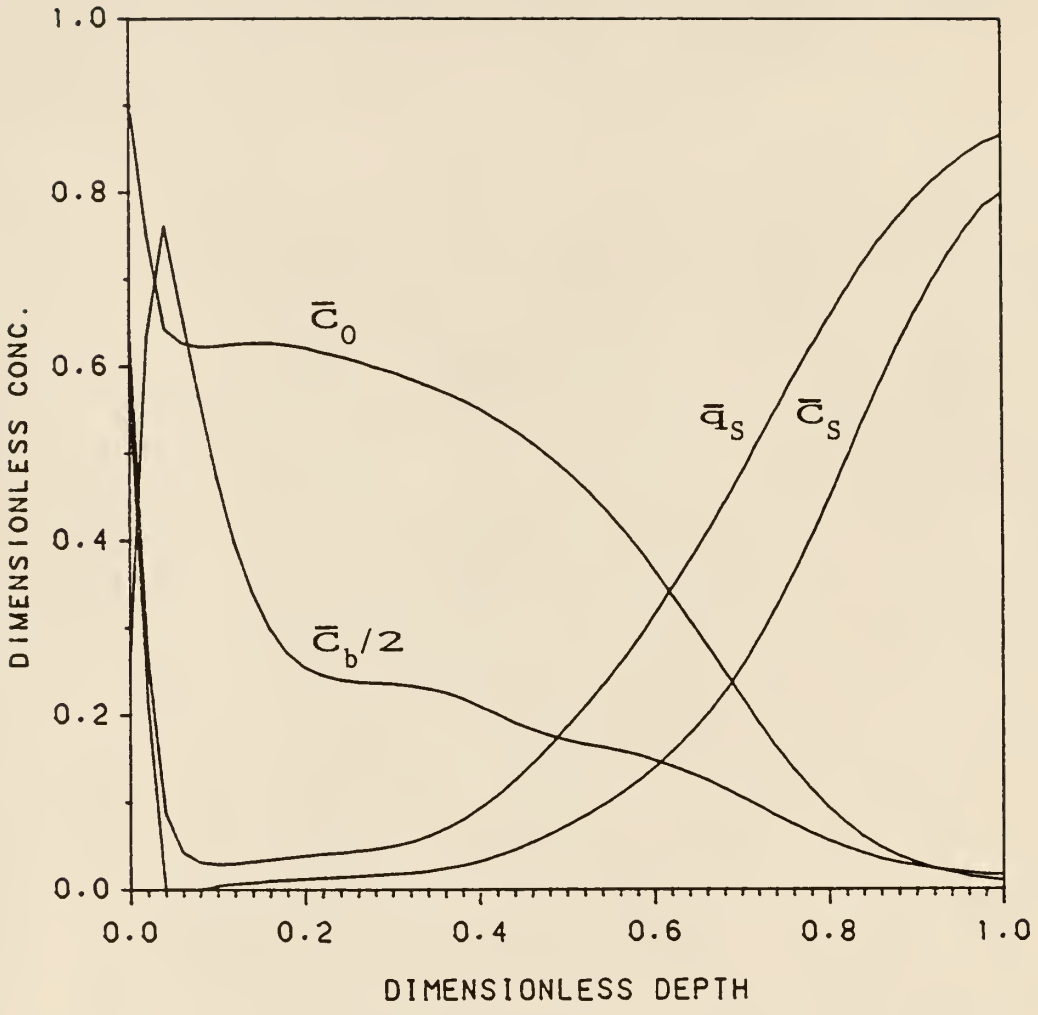

Figure 4.10. Concentration profiles for the recycle operation at Θ=6: Da'=0.2, R_s=20 and W=8.

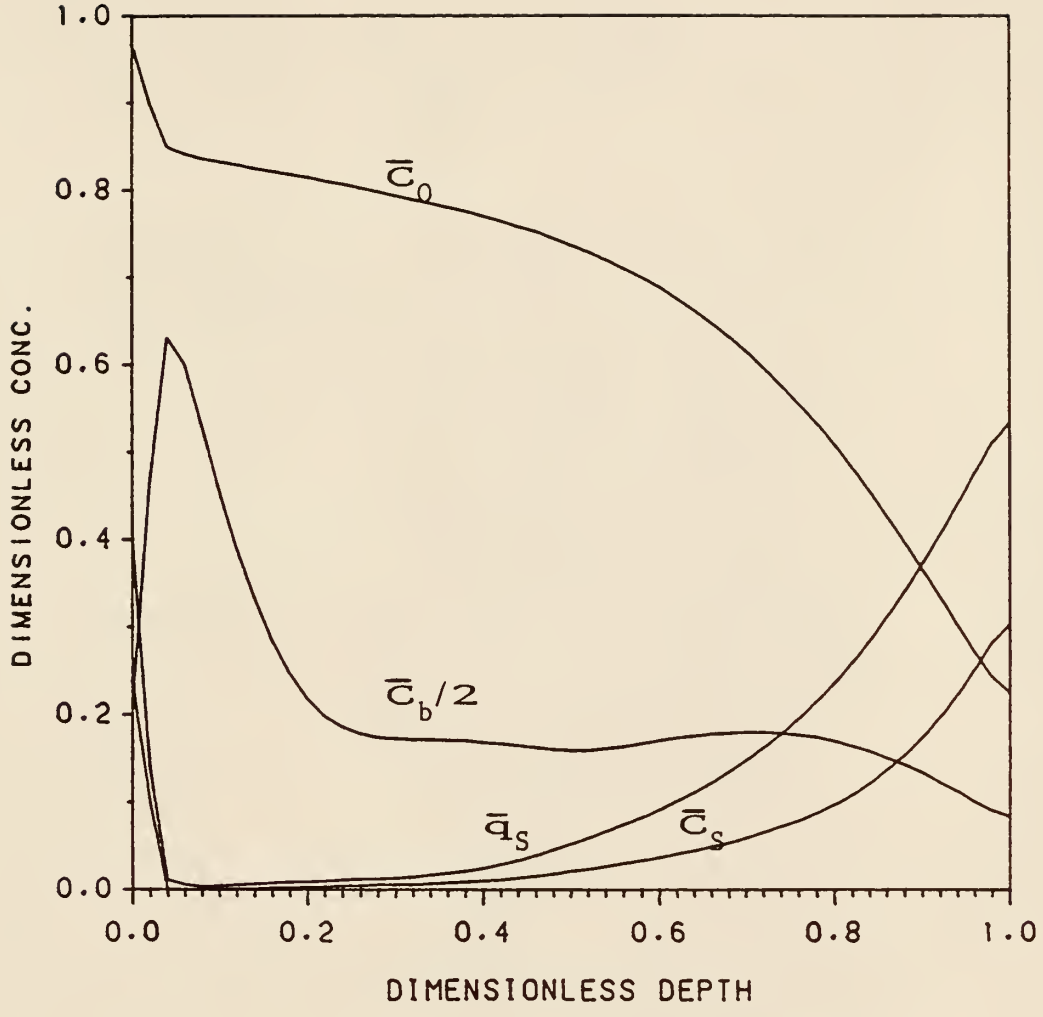

Figure 4.11. Concentration profiles for the recycle operation at θ=8: Da'=0.2, R_s=20 and W=8.

CHAPTER 5

CONCLUSIONS AND RECOMMENDATIONS

The major conclusions reached in the present thesis are recapitulated. This is followed by the presentation of recommendations for future work.

5.1 CONCLUSIONS

The present study has yielded the following significant conclusions.

1. A new finite difference method, the three-point backward finite difference method (TPB method), has been developed for solving a system of convection-dispersion PDE's, which have important applications in chemical and environmental engineering. This method can be applied to convection-dominated PDE's without significant numerical dispersion and oscillations, and to a system of convection-dispersion PDE's with coupled nonlinear reaction terms. Moreover, the method can be extended to a system of convection-dispersion PDE's coupled with ordinary differential equations (ODE's) or algebraic equations. Therefore, the present study provides a general numerical technique for solving various convection-dispersion models.

2. A mathematical model for in situ neutralization has been developed. The process, featuring fast reaction and relatively slow adsorption-desorption, gives rise to a nonequilibrium model. It comprises three governing differential equations, of which one is a convection-dominated partial differential equation (PDE) for base in the liquid phase, one is an ordinary differential equation (ODE) for base in the solid phase, and one is an ODE for acid in the solid phase. Dimensional analysis and numerical simulation have been conducted to investigate the effects of the model parameters on the concentration profiles, neutralization time, and extent of accumulation of base in the solid phase. Since an in situ neutralization process can be visualized as an in situ chemical treatment process, the model can be extended to any other nonequilibrium system in which a contaminant deposited in a soil bed is to be eliminated with another chemical agent.

3. A mathematical model for in situ biodegradation of contaminated soil has been developed. In this process, contaminants are initially deposited in a soil bed, and the rates of adsorption and desorption of contaminants are limited by transport within the pore network; thus, the local equilibrium assumption, widely used for simulation of in situ biodegradation of groundwater, is inappropriate. This observation gives rise to a nonequilibrium model

consisting of three PDE's and one ODE. The effects of insufficient oxygen supply, growth of biomass and transport resistance to contaminant migration on the rate of contaminant degradation have been examined by numerical simulation. The results indicate that the rate of biodegradation may be constrained not only by insufficient oxygen supply, but also by resistance to the contaminant migration. The effect of recycling the unreacted contaminants from the bottom of the bed to the top has also been examined through simulation, showing that biodegradation takes place mainly in the upper part of the bed.

5.2 RECOMMENDATIONS

The recommendations for future work are listed below.

1. Experiments are strongly suggested for evaluating model parameters. Four classes of parameters which are of particular interest are kinetic parameters, including all parameters appearing in the Monod model; equilibrium parameters, namely, adsorption-desorption equilibrium constants; hydraulic parameters, including the void fraction of the bed, the hydraulic conductivity determining the pore velocity of the liquid, and the density of the bed; and transport parameters, namely, the mass transfer

coefficients. The first two classes of parameters can be evaluated from batch experiments, and the third class can be obtained from experiments conducted in a soil column. The last class can be determined either from experiments or by fitting the computation results from the model simulation to the data from the column experiments.

2. The present model and numerical technique can be extended to develop a model for in situ biodegradation of contaminated soil in the unsaturated zone, where air is present in the soil bed. Consequently, the gas phase must be considered besides the liquid and solid phases. Biomass is not in the gas phase. In some applications, the vapor pressure of substrate is very low and the existence of substrate in the gas phase is negligible. Thus, only oxygen need be considered in the gas phase. If the transport of oxygen from the gas phase to the liquid phase is limited and oxygen in the gas phase is not in equilibrium with that in the liquid phase, an additional PDE for oxygen in the gas phase is required. Consequently, the model equations will consist of four PDE's and one ODE. If the existence of substrate in the gas phase is included and the concentration of substrate in the gas phase is in equilibrium with that in the liquid phase, the governing equation for substrate in the gas phase can be combined with that in the liquid phase. In this case, the number of equations will remain the same.

Stripping by air injection and biodegradation are considered simultaneously in this model. The TPB method developed in the present thesis can be applied to solve these equations.

3. The present model can also be extended to develop a nonequilibrium model for remediation of contaminated groundwater. For instance, almost all remediation of groundwater at contaminated sites is based on groundwater extraction by wells or drains, usually accompanied by treatment of the extracted water prior to disposal. This often causes an initial decrease in contaminant concentrations in the extracted water, followed by a leveling of concentration, and sometimes a gradual decline that is generally expected to continue over decades. This process was recently analyzed by Machay and Cherry (1989). They pointed out that dissolved organic contaminants generally move more slowly through granular aquifers than the groundwater itself because of sorptive interactions with the aquifer solids. However, they did not mention the effect of the slow rate of contaminant diffusion through the aquifer solid on contaminant desorption, which is often a rate-limiting factor and gives rise to nonequilibrium desorption. Thus, a nonequilibrium model is required.

4. The application of the concept of controlled release to in situ bioremediation is a promising subject (Fan, 1989). The controlled release of nutrients, such as oxygen

acceptors, and microorganisms can manipulate the concentration profiles and optimize the utilization of nutrients. Mathematical modeling of such a process can be based on the model developed in the present study and the nonequilibrium treatment of substrate in the present study can be extended to oxygen and biomass, though mass transfer models more sophisticated than the film model may be required to describe the controlled release of oxygen and biomass (Fan and Singh, 1989).

5. The rate of biodegradation of contaminants in soil is mainly controlled by the rate of their diffusion through soil particles, Thus, it may be advantageous to increase porosity of the soil bed and decrease the size of the soil particles by mechanical means when it is economically feasible to do so, e.g., when the soil bed is relatively shallow and highly impervious (Fan, 1989). Some of the mechanical means are drilling, filling, dynamiting, grinding and any combination of these.

REFERENCES

Fan, L. T., Private Communication, 1989.

Fan, L.T. and S. K. Singh, Controlled Release: a Quantitative Treatment, Springer-Verlag, Berlin, 1989.

Mackay, D. M. and J. A. Cherry, "Groundwater Contamination: Pump-and treat remediation," Environ. Sci. Technol., 23, 630-636 (1989).

APPENDIX I

DERIVATION OF THE EQUILIBRIUM MODEL

In this model, the concentration of each component in the liquid phase is in equilibrium with that of the corresponding component in the solid phase. Thus, for component i,

$$q_i = K_{di} C_i \tag{AI.1}$$

where a linear equilibrium isotherm is assumed. Substituting this equation into equation (4.4) in the text results in

$$\rho K_{di} \frac{\partial C_i}{\partial t} = a j_i^s \tag{AI.2}$$

Combining this equation with equation (4.6) in the text gives

$$\epsilon \frac{\partial C_i}{\partial t} + \rho K_{di} \frac{\partial C_i}{\partial t} = \epsilon E \frac{\partial^2 C_i}{\partial x^2} - \epsilon v \frac{\partial C_i}{\partial x} + \epsilon r_i^L + \rho r_i^{sf} - a J_i^s + a J_i^s \tag{AI.3}$$

or

$$\epsilon R_i \frac{\partial C_i}{\partial t} = \epsilon E \frac{\partial^2 C_i}{\partial x^2} - \epsilon v \frac{\partial C_i}{\partial x} + \epsilon r_i^L + \rho r_i^{sf} \tag{AI.4}$$

where

$$R_i = 1 + \frac{\rho K_{di}}{\epsilon}$$

This expression is the governing equation for the equilibrium model; note that no mass transfer term is involved.

APPENDIX II

DERIVATION OF EQUATIONS (4.24) THROUGH (4.26)

The procedures for deriving equations (4.24) through (4.26) in the text are the same. Thus, only equation (4.24) is derived here for illustration.

Substitution of equations (4.20) and (4.21) into equation (4.11) in the text gives

$$\epsilon\frac{\partial C_s}{\partial t} = \epsilon E\frac{\partial^2 C_s}{\partial x^2} - \epsilon v\frac{\partial C_s}{\partial x} + ak_s\left(\frac{q_s}{K_{ds}} - C_s\right) - \frac{\mu_m}{Y_s}\epsilon\, C_b\left(\frac{C_s}{K_s+C_s}\right)\left(\frac{C_o}{K_o+C_o}\right) - \frac{\mu_m}{Y_s}\rho\, q_b\left(\frac{C_s}{K_s+C_s}\right)\left(\frac{C_o}{K_o+C_o}\right) \qquad \text{(AII.1)}$$

Substituting equation (4.15) in the text into this equation and dividing both sides of resultant expression by ϵ yield

$$\frac{\partial C_s}{\partial t} = E\frac{\partial^2 C_s}{\partial x^2} - v\frac{\partial C_s}{\partial x} + \frac{k_s a}{\epsilon}\left(\frac{q_s}{K_{ds}} - C_s\right) - \frac{\mu_m}{Y_s}\left(1 + \frac{\rho K_{db}}{\epsilon}\right) C_b\left(\frac{C_s}{K_s+C_s}\right)\left(\frac{C_o}{K_o+C_o}\right)$$

or

$$\frac{\partial C_s}{\partial t} = E\frac{\partial^2 C_s}{\partial x^2} - v\frac{\partial C_s}{\partial x} + \frac{k_s a}{\epsilon}\left(\frac{q_s}{K_{ds}} - C_s\right) - \frac{\mu_m}{Y_s} R_b C_b\left(\frac{C_s}{K_s+C_s}\right)\left(\frac{C_o}{K_o+C_o}\right) \qquad \text{(AII.2)}$$

which is equation (4.24) in the text.

MODELING OF IN SITU NEUTRALIZATION AND BIODEGRADATION PROCESSES AND NUMERICAL SIMULATION WITH THE THREE-POINT BACKWARD FINITE DIFFERENCE METHOD

by

JIANCHU WU

B.S., Tianjin University, Tianjin, China. 1982

AN ABSTRACT OF A THESIS

submitted in partial fulfillment of the

requirement of the degree

MASTER OF SCIENCE

Department of Chemical Engineering

KANSAS STATE UNIVERSITY

Manhattan, Kansas

1989

Biodegradation has proven to be an effective method for remediation of contaminated soil. Modeling and simulation of in situ biodegradation processes have been conducted in the present thesis.

To facilitate the simulation, a three-point backward finite difference method (TPB method) has been developed for a system of convection-dispersion partial differential equations (PDE's). The method renders the second-order temporal and spatial accuracy and substantially reduces the numerical oscillations and diffusion. The resultant finite difference equations are solved with the tridiagonal matrix method at each time step. For a system of convection-dispersion PDE's with coupled nonlinear reaction terms, a two-step expansion technique is derived to linearize the finite difference equations and uncouple the PDE's. The accuracy of the expansion is of third order. Consequently, each PDE can be solved independently with the tridiagonal matrix method. Moreover, this method can be extended to a system of mixed PDE's coupled with ordinary differential equations and/or algebraic equations.

A model for in situ neutralization, which is often the first stage of in situ biodegradation, has been developed. The process, featuring fast reaction and relatively slow adsorption-desorption, gives rise to a nonequilibrium model comprising a convection-dispersion PDE for base in the

liquid phase, an ordinary differential equation (ODE) for base in the solid phase, and an ODE for acid in the solid phase. Dimensional analysis has been performed and numerical simulation has been conducted with the TPB method to investigate the effects of the model parameters on the concentration profiles, neutralization time, and extent of accumulation of base in the solid phase.

A model for in situ biodegradation of contaminants adsorbed in a soil bed has also been developed. The transport resistance to contaminant migration within the pore network in soil particles is considered. The model equations consist of three convection-dispersion PDE's and one ordinary differential equation. Dimensional analysis has been performed and numerical simulation has been conducted with the TPB method. The results show that the rate of biodegradation may be limited not only by insufficient oxygen supply, but also by transport resistance to the substrate desorption. Moreover, the simulation of the operation involving the recycle of unreacted contaminants has been conducted, indicating that biodegradation takes place mainly in the upper zone of the bed.